Ore Geology Reviews 86 (2017) 734–754

Contents lists available at ScienceDirect

Ore Geology Reviews

journal homepage: www.elsevier.com/locate/oregeo

Highly Siderophile Elements distribution, Os-S isotope systematics and U-Pb dating of mafic-ultramafic-hosted massive sulphide deposits (Southern Urals) – Implications on the sources of metals

Svetlana G. Tessalina [a,*], Elena Belousova [b]

[a] John de Laeter Centre for Isotope Research & The Institute for Geoscience Research (TIGeR), Faculty of Science and Engineering, Curtin University, Kent St, Bentley 6102, WA, Australia
[b] ARC Centre of Excellence for Core to Crust Fluid Systems (CCFS) and GEMOC National Key Centre, Department of Earth and Planetary Sciences, Macquarie University, Sydney, NSW 2109, Australia

ARTICLE INFO

Article history:
Received 16 December 2016
Received in revised form 8 February 2017
Accepted 20 March 2017
Available online 31 March 2017

Keywords:
Highly Siderophile Elements
Re-Os isotope systematics
S isotopes
Mafic-ultramafic hosted massive sulphide deposits
U-Pb zircon age
Urals

ABSTRACT

The behaviour of Highly Siderophile Elements (HSEs), including the Platinum Group Elements (PGEs), Re and Au, is still poorly known in hydrothermal systems due to their low concentrations in hydrothermal fluids and related ore deposits. In this work, HSE abundances were determined by fire assay and ICP-MS analyses in the Devonian Dergamysh and Ivanovka massive sulphide deposits from the Southern Urals, Russia. These deposits occur within mafic-ultramafic rocks of the Main Urals Fault suture zone, where the East-European continental unit comes into contact with the Magnitogorsk island arc system. Despite mafic-ultramafic host-rock compositions, the measured Pt and Pd contents are lower than those in island arc-hosted massive sulphide deposits from the same metallogenic province. In Dergamysh massive sulphides, the PGEs and Au positively correlate with Cu, whereas Pt also correlates with Co. For Ivanovka mainly disseminated ores and host rocks, two trends can be observed: (a) low to high PGE at low Au in rocks, with negative Ni-Pd correlation; and (b) both PGE and Au are variable in ores with significant correlation between Au and Pd. The Os-Pb-S isotope systematics in the seafloor Dergamysh hydrothermal system was mainly controlled by mixing of hydrothermal fluid with isotopic signature inherited from mafic host-rocks, and Devonian seawater. A possible additional contribution from more radiogenic Os component was attributed to older Precambrian rocks, which acquired radiogenic Os composition since their formation. Possible presence of such old rocks in serpentinitic melange was evidenced by U-Pb ages of zircons from Dergamysh deposit host rocks, ranging from 3.3 Ga to 507 Ma. These Archaean to Proterozoic zircons are consistent with source from the Volga-Uralia block of the East-European craton, adjacent to the Urals orogenic belt. Light sulphur isotopic composition in Dergamysh ores was attributed to bacterial reduction processes, which was also observed for modern serpentinite-hosted seafloor systems. Disproportionation of magmatic fluid however cannot be completely ruled out.

1. Introduction

The Highly Siderophile Elements (HSEs) include the Platinum Group Elements (PGEs: Pt, Pd, Ir, Ru, Rh, Os) plus Re and Au. Their behaviour is quite well known in magmatic systems, where it is mainly controlled by partial melting of mantle rocks and magmatic fractionation processes, but is still little understood in hydrothermal systems due to low elemental concentrations, which approach the detection limits of many analytical techniques. For example, the Os concentration in modern hydrothermal fluids is typically buffered at the seawater level, which is in the order of femtograms per litre (10^{-15} g/l; Sharma et al., 2000). Nevertheless, hydrothermal fluids may have an important role in the redistribution of HSEs within the continental crust and upper mantle. According to present crustal recycling models, the source of metals in hydrothermal fluids is usually considered to be the host volcanic and sedimentary rocks, with possible addition of magmatic fluid (e.g., Huston et al., 2010). The studies of hydrothermal deposits in modern oceanic settings have shown a range of Os isotopic compositions, which have been interpreted as the result of mixing of host rock-derived

* Corresponding author.
E-mail address: Svetlana.Tessalina@curtin.edu.au (S.G. Tessalina).

http://dx.doi.org/10.1016/j.oregeorev.2017.03.026
0169-1368/

(mainly MORB) and seawater-derived Os with $^{187}Os/^{188}Os$ close to 1 (Brügmann et al., 1998), with majority of massive sulphides from modern VHMS systems being close to the modern seawater composition in term of Os (Zeng et al., 2014). However, a contribution of metals from magmatic fluids into hydrothermal systems, including volcanic-hosted massive sulphide (hereafter VHMS) deposits from the Urals, was proposed by several authors based on melt and fluid inclusions studies (e.g., Karpukhina et al., 2013). A possible contribution from bacterial reduction processes was also inferred on the basis of the light sulphur isotopic compositions of some of the modern ultramafic-hosted hydrothermal systems (e.g., Delacour et al., 2008; Shanks, 2001).

The Dergamysh and Ivanovka VHMS deposits are situated within the Main Uralian Fault (thereafter MUF) zone, within an ophiolitic mélange dominated by mafic–intermediate volcanic rocks, serpentinites and volcanic-rich and siliceous sediments (e.g., Melekestseva et al., 2013). It was shown that these deposits were most likely formed in a supra-subduction zone setting based on the composition of serpentinite-hosted chromite (Tesalina et al., 2003) and on the geochemistry of associated igneous rocks (Nimis et al., 2010). The Re-Os isochron age (366 ± 2 Ma) of the Dergamysh ores (Gannoun et al., 2003) is at least 25 Ma younger than the Early Devonian biostratigraphic age of its hosting volcano-sedimentary sequence (Artyushkova and Maslov, 2008), and similar to that of subduction-related, high-pressure metamorphism of Proterozoic rocks from the margin of the former Baltica (East-European) continent (Beane and Connelly, 2000; Puchkov, 2010). However, good preservation of ore textures does not favour this hypothesis, and the younger Re-Os age may be alternatively attributed to multi-stage history of Urals VHMS deposits development as discussed in Tessalina et al. (2017).

In this paper, we examine the HSE (Pt, Pd, Os, Re, Au) abundances in the seafloor (Dergamysh) and sub-seafloor (Ivanovka) mafic-ultramafic hosted hydrothermal deposits, and discuss them in comparison with VHMS deposits in modern oceans and in Urals ancient island-arcs. Furthermore, previous Os and Pb isotope data and new S isotope data are used to assess the contributions of host rocks, seawater, magmatic versus subduction-related fluids and bacterial reduction processes to mafic-ultramafic-hosted hydrothermal systems in a supra-subduction zone oceanic setting. Seven new U-Pb zircon ages from the Dergamysh host rocks are presented for the first time, with application for metal sources and geodynamic development of the MUF zone.

2. Previous studies of HSE distribution in Urals VHMS deposits

In some VHMS deposits of the Urals, PGEs are a by-product of sulphide exploitation, encouraging a characterisation of their host mineral phases and distribution within the deposits. Analysis of Urals massive sulphide ores for PGEs was mentioned for the first time in 1936 by Zviaghenzev (unpublished report), who only indicated the presence of PGEs in the sulphide ores. Much later, Yushko-Zakharova (1975) reported Pt, Pd and Rh contents in chalcopyrite and bornite ores from some of the Central Urals sulphide deposits (Table 1). Novgorodova (1976) concluded that the Pd/Pt ratio increases from 0.2–0.7 to 1–9 and the Au/Ag ratio decreases from 0.2–0.1 to 0.06 in a given orebody from early pyrite-chalcopyrite to late barite-galena-sphalerite mineral assemblages. The same trend was observed from one orebody to another according to the degree of Cu-Zn-Pb enrichment and increase in the dacite-rhyolitic component in the volcanic host-rocks.

Volchenko et al. (1993) studied different ore types from four classic Uralian-type VHMS deposits, making several important observations: (1) the total PGE contents for these deposits vary from 0.1 to 1 ppm, averaging 0.3–0.5 ppm; (2) the PGE abundances in sulphide ores decrease in the order: Pt – Pd – Ru – Os – Ir; (3) pyrite ores are poor in Pd and total PGEs, which are enriched in chalcopyrite-bearing ores; (4) the Pt contents positively correlate with the Au contents (Table 1).

Dobrovolskaya and Distler (1998) reported on the PGE contents in massive sulphide ores and ore concentrates for five South Urals VHMS deposits (Table 1). They concluded that the PGE distribution depends on the type of host volcanic rock: low contents of Pt (up to 0.025 ppm) and Pd (up to 0.22 ppm) are found in deposits associated with bimodal basalt-rhyolite series (e.g., Sibai and Alexandrinka deposits); higher contents of Pt (up to 1.2 ppm) and Pd (up to 0.9 ppm) are associated with tholeiitic to calk-alkaline basalt-andesite-dacite series (e.g., Bakr-Tau, Tash-Tau, and Balta-Tau). The Rh content is also different but does not exceed 0.007 ppm in any of the deposits.

The highest value of Pt (2.9 ppm) was reported for the Pishminsko-Kluchevskoe VHMS deposit (Kontar and Libarova, 1997), which is hosted by mafic-ultramafic rocks (Table 1). The only PGE-bearing mineral reported in an Urals VHMS deposit is a melonite ($NiTe_2$) with up to 1.8% Pd from the Pishminsko-Kluchevskoe deposit (Eremin et al., 1997). Generally, the reported PGE values (dominated by Pt) do not exceed 1 ppm (Kontar and

Table 1
Contents (in ppb) of PGE in the Urals VHMS deposits.

Host rocks (type)	Deposit	N	Pt	Pd	Rh	Os	Ru	Pd/Pt	Reference
Mafic-ultramafic	Pyshminsko-Kluchevskoe	1	2900	NA	NA	NA	NA	NA	Kontar and Libarova (1997)
	Ivanovka	83	5	2	NA	0.78	NA	0.40	This work
	Dergamysh	26	5	4	NA	0.18	NA	0.80	This work
Bimodal (Urals)	Blyava	2	84	44	32	BDL	BDL	0.52	Yushko-Zakharova (1975)
	Karabash	2	BDL	20	BDL	BDL	BDL		Yushko-Zakharova (1975)
	Im.III International	1	21	33	30	BDL	BDL	1.57	Yushko-Zakharova (1975)
	Gai	6	306	94	7	9	25	0.30	Volchenko et al. (1993)
	Levikha gr.	7	94	28	12	31	97	0.30	Volchenko et al. (1993)
	Sibai	34	5	30	4	BDL	BDL	6.63	Dobrovolskaya and Distler (1998)
Felsic (Baimak)	Bakr-Tau	18	10	23	1	BDL	BDL	2.43	Dobrovolskaya and Distler (1998)
	Tash-Tau	5	417	334	4	BDL	BDL	0.80	Dobrovolskaya and Distler (1998)
	Balta-Tau	1	10	10	3	BDL	BDL	1	Dobrovolskaya and Distler (1998)
	Alexandrinskoe	12	13	45	1	0.29	BDL	3.53	Dobrovolskaya and Distler (1998)

Note: N – analyses number; NA – not analysed; BDL – bellow the detection limit. The median values are used for Dergamysh and Ivanovka deposits in this study. For other deposits, the average values are used.

Libarova, 1997). The mineralogy and deposition conditions of noble metals in Urals VHMS deposits have been also discussed recently in Vikentev et al. (2002, 2004, 2006), Kovalev et al. (2015) and references therein. They concluded that the majority of Au and some PGEs contents are hosted by pyrite; the remainder is enriched in the products of the latest paragenesis.

The Re-Os elemental and isotope composition of Dergamysh and Ivanovka ores have been described previously by Gannoun et al. (2003). At Dergamysh, the Re contents are highly variable, ranging from 1 to 41 ppb, whereas at Ivanovka they are near the low end of this interval, ranging from 1 to 6 ppb (Gannoun et al., 2003). The distribution of Au in the studied deposits was discussed by Nimis et al. (2008) and Melekestseva et al. (2013). At Ivanovka, Au shows no evident correlation with other metals (Nimis et al., 2008). In the Dergamysh main orebody, Au shows only a weak correlation with Cu (Melekestseva et al., 2013).

The lead isotopic compositions of Dergamysh and Ivanovka ores are comparable to that of the Ordovician MORBs, derived from highly depleted mantle metasomatised during dehydrational partial melting of subducted slab and oceanic sediments (Tessalina et al., 2016a).

3. Geological setting and sampling strategy

3.1. Regional geology

The Urals is an orogenic belt of 2000 km in length, which marks the geographic boundary between Europe and Asia. The Urals belt was formed as a result of intra-oceanic subduction, island arc formation and subsequent collision of the arc with the East European (Laurussia) and Kazakhstan continents (Borodaevskaya et al., 1977; Zonenshain et al., 1984; Koroteev et al., 1997; Brown et al., 2001; Seravkin et al., 1994; Zaykov et al., 1996; Herrington et al., 2002; Puchkov, 2010). The structure of the Urals, and in particular that of the Southern Urals, is well preserved. The following subdivisions can be made (Fig. 1):

(1) The Main Urals Fault (MUF) is a 10–20 km wide suture zone, which separates the metamorphic units of the Ural–Tau tectonic zone from the volcanic complexes of the Tagil–Magnitogorsk–Mugodzhary island–arc systems (Fig. 1). The MUF is underlain by crystalline rocks of the East-European continent (e.g., Puchkov, 2010). It mostly consists of a serpentinitic mélange, which contains up to 4-km large blocks of Ordovician to Carboniferous igneous and sedimentary rocks (largely derived from the island arc) and a number of slabs of ultramafic rocks and massifs. The mafic-ultramafuc massifs have been subdivided into three main types: (1) lherzolite-harzburgite complexes (e.g., Tessalina et al., 2007); (2) zoned dunite-clinopyroxenite-gabbro complexes (Urals-Alaskan type) in the Middle Urals Platinum belt (e.g., Tessalina et al., 2016b); and (3) harzburgite-dunite-volcanics ophiolite complexes in the Southern Urals (Savelieva et al., 1997). Development of the MUF went through several stages that were linked to the formation of the Palaeozoic Urals belt (Spadea et al., 2002; Brown and Spadea, 1999). These stages include: (1) oceanic crust formation (Ordovician–Silurian); (2) intra-oceanic subduction with formation of island arc complexes and deposition of siliciclastic and flyschoid sediments and olistostromes (Early-Middle Devonian); (3) early collision between island arcs and the East-European continent (Late Devonian–Early Carboniferous); and (4) late collision between the East-European and Kazakh continents (Middle Carboniferous–Early Permian) (Brown and Spadea, 1999; Puchkov, 2010).

(2) The Magnitogorsk island arc zone, consisting of Devonian volcanic and sedimentary rocks. An intermediate "inter-arc" basin, filled by Late Devonian-Lower Carboniferous volcanic and sedimentary rocks, divides the Magnitogorsk structure into the West- and East-Magnitogorsk zones;

(3) Sakmara zone, consisting of several tectonic sheets, composed of bathyal sediments of the continental margin (Puchkov, 2010), overlain by Ordovician and Devonian island arc complexes and ophiolites. Its tectonic structure however is not clear (see Tessalina et al., 2017 for more details). Recent fauna dating (Dubinina and Ryazantsev, 2008) indi-

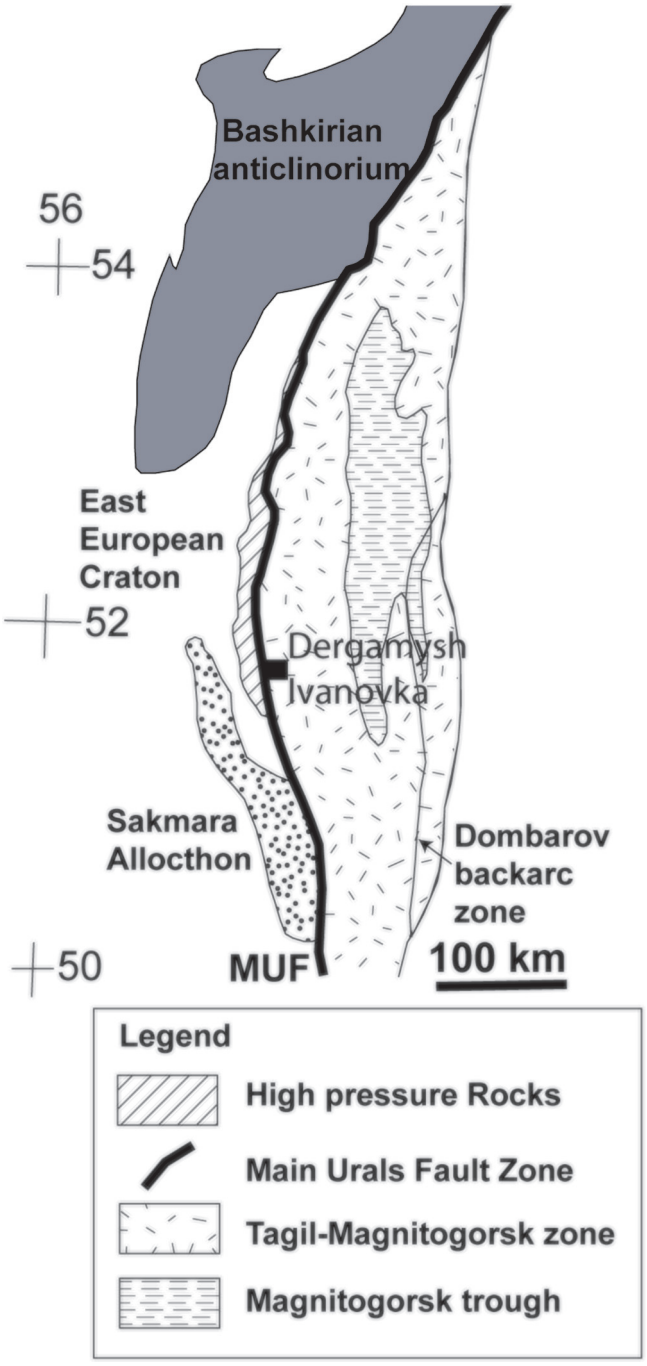

Fig. 1. Simplified geological map of the Southern Urals showing the main island arc structures and location of the Dergamysh and Ivanovka VHMS deposits (modified after Herrington et al., 2005).

cated a Late Ordovician age and suggests that the Sakmara volcanics are linked to the Ordovician Guberlya arc (Puchkov, 2010, 2017).

(4) The southern part of the MUF contains three mafic-ultramafic-hosted massive sulphide deposits, including the Ishkinino, Dergamysh and Ivanovka deposits studied here (Tessalina et al., 2001; Nimis et al., 2004, 2008, 2010; Melekestseva et al., 2013). The study of relict chromites in ores from the Ishkinino and Ivanovka deposits, and the geochemical analysis of associated igneous rocks, have shown that the massive sulphides were formed in a supra-subduction zone setting (Tessalina et al., 2003; Nimis et al., 2010).

3.2. Dergamysh deposit

The host rocks of the Dergamysh deposit belong to a sequence of mafic and ultramafic rocks within the southern part of the MUF suture zone (Fig. 1). The deposit occurs within a synform composed of several tectonic sheets (Melekestseva et al., 2013). Six of them have been recognised by Melekestseva et al. (2013) and briefly described here from the bottom to the top: (1) olistoliths of various composition; (2) brecciated serpentinite hosting the massive sulphide orebody, intruded by gabbro; (3) brecciated serpentinite, blocks of talc–carbonate rocks and gabbros; (4) volcanoclastic sediments, with interlayers of carbonaceous siltstones, sandstones and serpentinites; (5) volcanic rocks of andesitic to dacitic compositions (Fig. 2).

The main orebody is a 6–40 m-thick sulphide mound made of colloform and brecciated pyrite-marcasite-chalcopyrite ores (Melekestseva et al., 2013). The mound consists of two to three stacked lenses intercalated with thin layers of brecciated serpentinites and chloritized mafic rocks. The mineralisation is represented by several ore intervals, which are characterized by dominant pyrite and variable proportions of marcasite, chalcopyrite and sphalerite. Most ore intervals display a clastic texture, locally with distinct rhythmically graded bedding and abundant concretionary, colloform and framboidal aggregates of pyrite-marcasite (Melekestseva et al., 2013). Rare pyrrhotite relicts, mostly replaced by pyrite–marcasite or pyrite–magnetite aggregates, were found in a single massive layer. Main gangue minerals are talc, carbonate, quartz and chlorite.

3.3. Ivanovka deposit

The Ivanovka deposit is located near the E-dipping western margin of the MUF suture zone (Figs. 1 and 3). It consists of several densely packed ore lenses and layers within a largely brecciated, up to 100–150 m-thick mafic-ultramafic sequence (Tesalina et al., 2003; Melekestseva et al., 2013). The main host-rock lithologies consist of hydrothermally-altered mafic and ultramafic rocks, which included olivine-rich melagabbroids, gabbros, dolerites, basalts and mantle peridotites. The ore-bearing rock sequence lies conformably between a footwall serpentinite and overlying pillow-basalts. The geochemistry of associated igneous rocks supports an Early Devonian age for the mafic-ultramafic complex that is host to the deposits (Nimis et al., 2010), consistent with post-Silurian biostratigraphic dating of conglomeratic interlayers (Seravkin et al., 2001). The sulphide mineralization comprises massive, stockwork and disseminated ores consisting of pyrrhotite ± pyrite ± chalcopyrite assemblages, locally with chalcopyrite–cubanite intergrowths (Melekestseva et al., 2013). The uppermost ore level is characterized by network-like aggregates of lamellar pyrrhotite with interstitial Mg-rich saponite, chlorite, Fe-rich talc, quartz or dolomite (Nimis et al., 2004), resembling textures found in some modern seafloor hydrothermal mounds (e.g. Goodfellow and Franklin, 1993; Zierenberg et al., 1993).

4. Sample materials and analytical methods

Whole-ore samples used for this study were taken from two drill cores cross-cutting the Dergamysh orebody and the Ivanovka mineralized sequence. Samples from the Dergamysh deposit were collected from the purposely drilled core 1T (see Fig. 2 for drill core location), which cross-cut the central portion of the main orebody and reached the base of the second massive lens at a depth of 78 m. A detailed stratigraphic description of this drill core is given in Melekestseva et al. (2013). The samples include 30 core intervals, each about 1 m long, and 10 chip samples. Samples from the Ivanovka deposit were collected from drill core 2T (Fig. 3) described in Tesalina et al. (2003) and include 44 core intervals

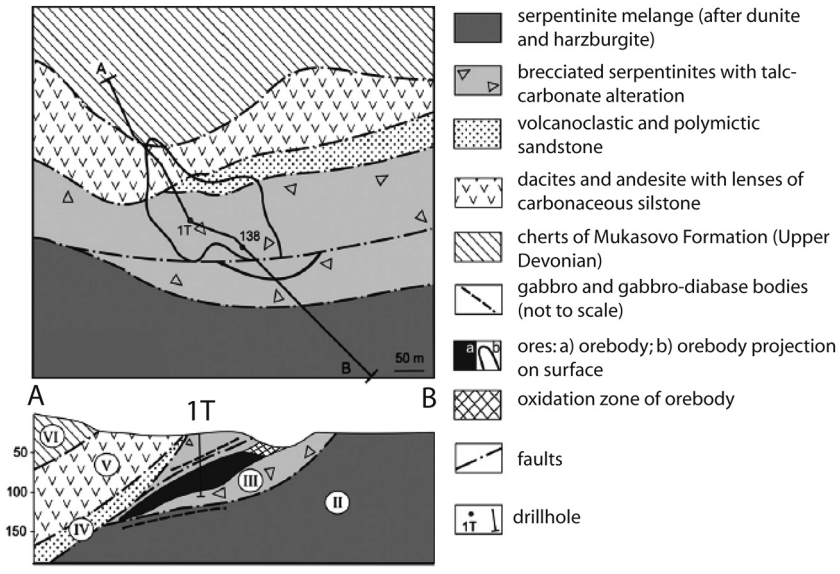

Fig. 2. Geological map and cross-section across the Dergamysh deposit (adapted from Melekestseva et al., 2013). The location of drillhole T1 is shown. The tectonic sheets are described in the text. Note that tectonic sheet 1 is not exposed in the deposit area.

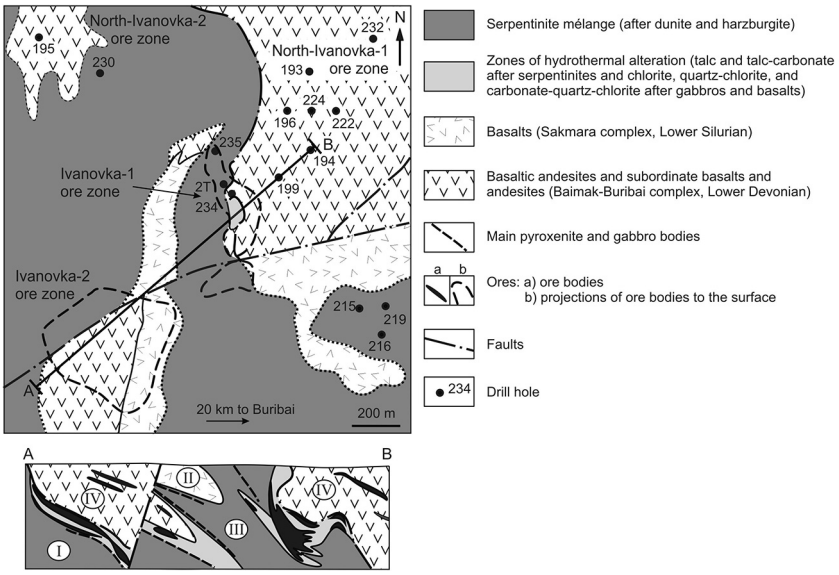

Fig. 3. Geological map and cross-section of the Ivanovka deposit (from Melekestseva et al., 2013).

Table 2
Contents of the main (Cu, Zn, S) and trace (Co, Au, Pt, Pd) elements in drillhole 1T (see Fig. 1 for location) through the Dergamysh orebody. These data were previously reported in graphical form by Nimis et al. (2008; Fig. 8) and Melekestseva et al. (2013; Figs. 7 and 8).

Interval		Lithology	Main	Cu	Zn	S	Co	Ni	Au	Pt	Pd
From	To		Ore	%	%	%	%	%	ppb	ppb	ppb
45.3	46.3	Chl		0.19	0.10	2.67	0.027	0.053	133	<10	9
46.3	47.3	Sand	Py	4.27	0.49	37.97	0.007	0.014	5070	<10	22
47.3	48.3	Sand	Py	2.65	0.10	38.86	0.157	0.013	4670	48	13
48.3	49.3	Sand	Py	4.58	0.45	40.81	0.251	0.009	6170	54	23
49.4	49.8	Serp		2.86	1.83	17.38	0.09	0.078	1490	27	7
49.8	50.8	Sand	Py	1.40	0.03	33.41	0.006	0.009	531	24	2
50.8	51.8	Sand	Py	2.58	0.53	29.33	0.235	0.011	912	18	3
51.8	52.8	Sand	Py	1.37	0.04	29.59	0.238	0.018	119	<10	<1
52.8	53.8	Sand	Py	1.01	0.06	30.36	0.115	0.007	460	<10	7
53.8	54.8	Sand	Py	0.96	0.15	24.23	0.125	0.009	239	<10	3
54.8	55.8	Sand	Py	2.08	0.57	32.76	0.201	0.010	1450	16	9
55.8	56.8	OrBr	Py	1.77	0.27	32.86	0.207	0.028	1280	<10	13
56.8	57.8	OrBr	Py	1.15	0.59	31.85	0.159	0.011	604	<10	8
57.8	58.8	ElBr	Py	2.26	0.57	33.42	0.251	0.016	793	<10	7
58.8	59.8	ElBr	Py	1.86	0.31	33.95	0.146	0.014	1280	<10	8
59.8	60.8	ElBr	Py	1.46	1.00	40.13	0.136	0.009	680	<10	4
60.8	61.8	ElBr	Py	1.00	1.12	38.35	0.138	0.010	480	15	3
61.8	62.8	ElBr	Py	0.67	0.77	40.61	0.057	0.006	648	<10	4
62.8	63.8	ElBr	Py	1.08	1.24	41.09	0.144	0.006	503	12	4
63.8	64.8	ElBr	Py	1.31	0.81	41.05	0.118	0.005	664	20	12
64.8	65.8	ElBr	Py	1.27	0.35	48.26	0.115	0.005	407	20	4
65.8	66.8	ElBr	Py	1.27	0.43	36.36	0.134	0.005	576	<10	3
66.8	67.8	OrBr	Py	1.05	0.37	37.43	0.104	0.012	436	<10	<1
67.8	68.8	OrBr	Py	1.23	0.66	38.27	0.129	0.010	832	<10	<1
68.8	69.8	Sand	Py	1.12	0.62	36.67	0.109	0.010	936	<10	6
69.8	70.8	ElBr	Py	1.45	0.25	34.72	0.194	0.009	345	<10	3
70.8	71.8	ElBr	Py	1.71	0.19	36.41	0.187	0.008	668	29	4
71.8	72.8	Sand	Py	1.60	0.24	37.08	0.238	0.064	243	24	<1
72.8	73.8	Sand	Py	1.48	0.20	42.23	0.087	0.031	420	<10	<1
73.8	74.8	Sand	Py	0.99	0.17	31.56	0.159	0.031	195	<10	<1
74.8	75.8	OrBr	Py	1.15	0.24	20.79	0.167	0.026	162	<10	<1
75.8	76.8	Sand	Py	1.47	0.13	39.7	0.089	0.008	1520	19	4
76.8	77.8	Serp		0.36	0.04	14.26	0.046	0.051	94	<10	1
Median				1.37	0.35	36.36	0.14	0.010	604	5.00	4.00

Note. For calculations of median values, the ½ of the detection limit is used. The abbreviations for different lithology types are: Serp - serpentinite; Chl – chlorite-quartz altered basaltic breccia; OrBr – ore breccia; ElBr – eluvial (*in-situ*) breccia with big ore clasts (up to 0.5 m); Sand – pyrite sandstone; Py – pyrite.

approximately 1 m long. Concentrations of Au, Co, Ni, Cu, Zn and S in the same core intervals from Dergamysh and Ivanovka were discussed and reported in graphical form by Nimis et al. (2008) and Melekestseva et al. (2013). These data are reported here in full for the first time along with additional data for Pt and Pd (Tables 2 and 3) and previously unreported, detailed information on the analytical methods used. Additional main and trace element analyses for 8 chip samples, and sulphur isotope analyses for 10 chip

Table 3
Contents of the main (Cu, Zn, S, Co, Ni) and trace (Au, Pt, Pd) elements in drillhole 2T through the Ivanovka deposit. These data were previously reported in graphical form by Nimis et al. (2008; Fig. 8) and Melekestseva et al. (2013; Figs. 7 and 8).

Interval		Litho	Main	Cu	Zn	S	Co	Ni	Au	Pt	Pd
From	To		Ore	%	%	%	%	%	ppb	ppb	ppb
78.6	79.6	Talc		0.02	<0.01	1.24	0.010	0.134	33	<10	4
79.6	80.6	Cc		0.02	0.01	2.50	0.025	0.491	96	<10	1
80.6	82.2	Mas	Po-Py	0.64	0.01	31.62	0.055	0.188	176	<10	8
82.2	83.2	UMBr		0.13	0.01	7.59	0.036	0.462	118	<10	5
83.2	84.2	UMBr		0.02	<0.01	1.50	0.014	0.208	24	<10	1
84.2	85.7	UMBr		<0.01	0.02	0.36	0.011	0.108	9	<10	<1
85.7	86.2	Mas	Po	1.48	0.02	19.75	0.043	0.126	5360	23	13
86.2	87.2	UMBr		0.01	<0.01	1.04	0.009	0.100	18	<10	<1
87.2	88.2	Dis	Po + Py	0.08	0.02	14.99	0.011	0.100	137	<10	2
88.2	89.2	Dis	Po + Py	0.05	<0.01	10.16	0.009	0.072	192	<10	2
89.2	90.5	Pegm	Po	0.11	0.01	9.67	0.012	0.047	52	<10	1
90.5	91.5	UMBr		0.05	0.02	0.67	0.013	0.125	57	12	5
91.5	92.5	UMBr		0.01	<0.01	1.48	0.008	0.139	19	<10	2
92.5	93.5	UMBr		0.01	<0.01	0.56	0.009	0.158	55	<10	2
93.5	94.5	UMBr		<0.01	<0.01	0.39	0.008	0.253	9	<10	<1
94.5	95.5	UMBr		<0.01	<0.01	0.29	0.009	0.167	7	<10	1
95.5	96.5	UMBr		<0.01	<0.01	0.28	0.009	0.163	5	<10	2
96.5	97.5	UMBr		<0.01	<0.01	0.20	0.007	0.129	4	<10	3
97.5	98.5	UMBr		<0.01	0.01	0.63	0.008	0.147	14	18	4
98.5	99.5	UMBr		0.02	0.07	3.04	0.011	0.123	13	<10	<1
99.5	100.2	UMBr		0.02	<0.01	3.28	0.009	0.169	21	<10	<1
100.2	101.5	Pegm	Po	0.14	0.03	20.41	0.023	0.106	42	<10	1
101.5	102.5	Pegm	Po	0.05	0.02	5.88	0.013	0.150	25	15	<1
102.5	103.5	UMBr		0.01	0.01	2.81	0.009	0.157	17	<10	<1
103.5	104.5	UMBr		0.01	<0.01	1.75	0.009	0.200	8	<10	<1
104.5	105.5	UMBr		<0.01	<0.01	0.62	0.007	0.111	10	<10	<1
105.5	106.5	UMBr		<0.01	<0.01	0.34	0.008	0.169	1	<10	<1
106.5	107.5	UMBr		<0.01	<0.01	0.57	0.010	0.176	3	<10	1
107.5	108.5	UMBr		<0.01	<0.01	0.51	0.010	0.184	6	<10	<1
108.5	109.5	UMBr		<0.01	<0.01	0.33	0.010	0.160	3	<10	<1
109.5	110.5	UMBr		<0.01	<0.01	0.30	0.010	0.167	6	34	6
110.5	111.5	UMBr		<0.01	<0.01	0.46	0.010	0.128	9	12	7
111.5	112.5	UMBr		<0.01	<0.01	0.36	0.007	0.157	8	10	3
112.5	113.5	UMBr		<0.01	<0.01	0.19	0.008	0.166	2	14	<1
113.5	114.5	UMBr		<0.01	<0.01	0.21	0.009	0.172	3	10	<1
114.5	115.5	UMBr		<0.01	<0.01	0.44	0.010	0.175	6	<10	<1
115.5	115.9	Pegm	Po	0.31	<0.01	22.53	0.051	0.159	58	<10	<1
115.9	116.9	UMBr		<0.01	<0.01	0.90	0.011	0.192	7	16	<1
116.9	117.9	UMBr		0.01	<0.01	1.37	0.010	0.159	5	24	<1
117.9	118.9	Pegm		0.03	<0.01	8.40	0.007	0.060	6	<10	<1
118.9	120.4	UMBr		0.04	<0.01	3.14	0.010	0.153	21	<10	<1
120.4	121.4	Mas	Po + Py	0.14	<0.01	16.43	0.022	0.131	294	15	4
121.4	122.4	Mas	Po + Py	0.17	<0.01	23.99	0.020	0.135	776	13	<1
122.4	123.4	Mas	Po + Py	0.2	0.09	24.24	0.017	0.141	1600	<10	<1
123.4	124.8	Dis	Po + Py	0.02	0.06	6.02	0.011	0.142	123	<10	<1
124.8	125.8	Pegm	Po	<0.01	<0.01	0.72	0.009	0.132	9	<10	<1
125.8	126.8	Pegm	Po	<0.01	<0.01	1.01	0.010	0.115	16	<10	1
126.8	127.8	Pegm	Po	0.1	0.21	17.81	0.014	0.145	400	<10	<1
127.8	128.8	Pegm	Po	0.18	0.11	26.52	0.017	0.132	1270	<10	<1
128.8	129.9	Mas	Po + Py	0.56	0.02	12.97	0.032	0.077	168	<10	2
129.9	130.5	Dis	Po + Py	0.03	<0.01	3.49	0.014	0.067	50	<10	<1
130.5	131.7	Mas	Po + Py	1.52	0.02	30.87	0.079	0.138	238	11	7
131.7	132.9	Mas	Po + Py	1.16	0.01	29.30	0.235	0.166	746	<10	7
132.9	134	Chl		0.02	<0.01	2.53	0.013	0.039	28	<10	12
134	135	Chl		0.01	<0.01	2.28	0.013	0.045	89	20	9
135	136	Chl		<0.01	<0.01	0.59	0.009	0.030	10	<10	11
136	137.4	Chl		0.04	<0.01	5.14	0.015	0.045	72	14	12
137.4	138.9	Chl		0.03	0.01	4.45	0.012	0.050	250	20	12
138.9	139.9	Mas	Po + Py	0.25	0.03	32.89	0.016	0.141	940	70	4
139.9	140.9	Dis	Po	0.19	0.06	26.24	0.016	0.155	2300	19	10
140.9	141.9	Dis	Po	0.19	0.07	29.70	0.016	0.189	1480	<10	10
141.9	143.2	Pegm	Po	0.15	0.13	21.69	0.016	0.161	1340	12	6
143.2	144.2	Chl		<0.01	<0.01	0.64	0.014	0.048	21	<10	18
144.2	145.2	Chl		<0.01	<0.01	0.53	0.014	0.021	16	<10	15
145.2	146.2	Chl		<0.01	<0.01	0.21	0.012	0.026	5	<10	15
146.2	147.2	Chl		<0.01	<0.01	0.23	0.012	0.021	21	<10	14
147.2	148	Chl		0.02	<0.01	0.75	0.017	0.024	67	<10	14
148	149.6	Mas	Po	0.82	<0.01	33.76	0.050	0.151	3730	12	14
149.6	150.2	Dis	Po	0.18	<0.01	12.45	0.027	0.064	992	<10	9
150.2	151.2	Dis	Po + Py	0.28	<0.01	23.78	0.037	0.134	250	<10	<1
151.2	152.2	Mas	Po + Py	0.68	<0.01	30.66	0.054	0.141	600	<10	1
152.2	153.2	Mas	Po + PY	0.49	<0.01	30.16	0.070	0.145	624	<10	<1
153.2	154.2	Dis	Po + Py	0.44	<0.01	27.64	0.030	0.164	653	<10	<1

(*continued on next page*)

Table 3 (*continued*)

Interval		Litho	Main	Cu	Zn	S	Co	Ni	Au	Pt	Pd
From	To		Ore	%	%	%	%	%	ppb	ppb	ppb
154.2	155.2	Dis	Po + Py	0.28	<0.01	28.63	0.033	0.143	520	<10	2
155.2	156	Dis	Po + Py	0.4	0.02	32.75	0.044	0.138	427	<10	2
156	156.6	Chl		0.29	<0.01	2.58	0.017	0.020	24	<10	15
156.6	157.6	Dis	Po + Py	0.33	<0.01	26.10	0.029	0.224	58	<10	<1
157.6	158.8	Dis	Po + Py	1.13	0.01	28.58	0.076	0.162	177	<10	<1
158.8	159.8	Chl		0.06	<0.01	6.56	0.016	0.086	116	<10	5
159.8	160.3	Dis	Po + Py	3.40	0.04	31.23	0.077	0.159	420	<10	<1
160.3	161.4	Chl		0.07	<0.01	1.92	0.015	0.038	25	<10	8
161.4	162.4	Dis	Po + Py	0.24	<0.01	15.90	0.035	0.120	250	<10	3
162.4	163.4	UMBr		0.06	<0.01	4.51	0.013	0.125	22	23	11

Note. The abbreviations for different lithology types are: Serp - serpentinite; Chl – chlorite-altered mafic rocks; Dis – disseminated ores; Mas – massive ores; Pegm – ''pegmatoid' pyrrhotite; UMBr – polygenic altered breccia with ultramafic and mafic clasts; Cc – serpentinite breccia completely altered into carbonate-smectite; Chl – chlorite-altered rocks after mafic protoliths; Po – pyrrothite; Py – pyrite.

samples from the Dergamysh drill core 1T are also provided (Tables 4 and 5). These chip samples are a subset of those that were previously analysed for Re and Os isotopes by Gannoun et al. (2003).

Sample for U-Pb study has been collected by I.Yu.Melekestseva in Dergamysh open pit in 2014 (coordinates N 51°53′55.3″, E 58°01′47.4″). It was taken from the lavo-clastite horizon of andesitic composition near the contact with serpentinites.

4.1. HSE analysis

Whole-ore samples from the homogenised 1 m-long core intervals were analysed for Au, Pt and Pd at SGS Laboratory, Toronto (Canada), using a lead collection fire assay technique. The pulverised sample was weighed and mixed with a fluxing agent and lead as a collector. This mixture was heated up to 1000° C for 20 min, enabling the sample to fuse with separation of precious metals and lead from the silicate slag to form a button (containing the precious metals) in the bottom of the crucible. After cooling, the lead button was separated from the silicate slag and precious metals were extracted by a process known as cupellation. During cupellation, the lead in the button oxidises and is absorbed into the cupel leaving a precious metal bead known as a prill, which is then dissolved in *aqua regia* (mixture of hydrochloric and nitric acids) and analysed by inductively-coupled plasma mass spectrometry (ICP-MS). The detection limit for Au, Pt and Pd was better than 1, 10 and 1 ppb, respectively. The relative precision and accuracy were better than 5% for all elements.

Table 4
Contents of main (Fe, Zn) and trace metals (Co, Ni, As, Sb, Mo, U, Se, Au, Ag, Os, Re) in the chip samples from the Dergamysh deposit.

ID	Lith	Fe	Zn	Se	U	Co	Ni	As	Sb	Mo	Au	Ag	Re	Os	Os_c[a]
Units		%	ppm								Ppb			ppt	
D21	Serp	6.4	50	bdl	bdl	72	878	0.67	bdl	bdl	bdl	bdl	bdl	NA	NA
D45.1	Chl-Q	10.5	166	0.77	0.8	38	103	1.85	1.1	bdl	4.5	Bdl	0.97	24	22
D46.3	Sand	41.8	1350	41.6	7.4	2465	91	47.5	61.3	12.2	1895	13,320	8.71	106	76
D50.7	Br	33.4	3888	26.9	2.2	1538	27	60.8	19.2	14.6	214	630	38.58	205	57
D59	Br	43.9	487	35.3	3	2041	32	27.9	2.6	3.56	285	Bdl	11.97	67	21
D67.1	Br	42.5	5370	29.2	1.5	1723	80	355	50.2	12	1012	880	38.61	227	74
Duplicate		NA	NA	NA	NA	NA	NA	NA	NA	NA	NA	NA	36.86	327	176
D70.1	Br	42.2	267	65.3	3.7	2223	64	265	21.7	5.3	127	bdl	18.33	81	11

Chl-Q – pillow-hyaloclastite breccia altered to chlorite-quartz with disseminated sulphides.
Notes: Numbers in sample labels refer to sample depth along the drillhole.
Bdl refers to Below Detection Limit (see Method section for detection limits value); NA – not analysed.
[a] Common Os (Os_C) represents the contents of Os at the moment of Re-Os system closure (time zero). It is calculated by substraction of radiogenic ^{187}Os from total Os contents.

Table 5
The Os isotope composition (data from Gannoun et al., 2003; initial $^{187}Os/^{188}Os$ ratio calculated at 366 Ma) and S isotope composition (this work) for the selected massive sulphide samples from Dergamysh deposit. Abbreviations used: Mc – marcasite, Py – pyrite, Po – pyrrhotite, Serp –serpentinite; Sand – sulphide sandstone; Br – ore breccia; DMM – depleted mantle; D – Devonian.

Sample ID	Depth	Lithology	Composition	Special notes	$^{187}Os/^{188}Os$ initial at 366 Ma	δ34S, ‰
D45.8	45.8	Sand	Mc-Py	Po relics	0.56	−3.3
D46.3	46.3	Sand	Mc-Py		0.38	−3.2
D47.5	47.5	Sand	Py-Mc		0.72	−3.9
D56.7	56.7	Sand	Mc-Py + Serp	Po relics	0.21	−2.1
D59a	59	Br	Py	Po relics	1.56	1
D59.7	59.7	Br	Py	Po relics	1.76	−4.6
D62.5	62.5	Br	Py		1.48	−3.3
D67a	67	Br	Mc-Py		0.62	−2.2
D70a	70	Br	Mc-Py		4.33	1.3
D71.7	71.7	Br	Mc-Py		1.39	0.7
DMM					0.12	−1.3
D seawater				0.2	19	

4.2. Trace elements in Dergamysh ores

The concentrations of main (Fe, Zn) and selected trace metals (Co, Ni, As, Sb, Mo, U, Se, Au, Ag, Os, Re) in 8 whole-ore chip samples from the Dergamysh drill core 1T (Table 4) were determined by ICP-MS at the Service d'Analyse des Roches et des Minéraux (SARM), Centre de Récherche Pétrographiques et Géochimique (SRPG-CNRS, Nancy, France). The analyses show variable precision and accuracy, which strongly depend on element concentration in the samples. At a concentration level above 1 ppm (i.e., for most analysed elements except Au, Ag, Re and Os), the relative precision and accuracy are better than 15%. Analyses for the international standards used as well as the analytical procedures used in the CRPG laboratory at Nancy can be downloaded from the website at http://www.crpg.cnrs-nancy.fr/SARM/index.html.

4.3. Sulphur isotopes

For sulphur isotope analyses, sulphide samples were crushed and small pyrite particles were hand-picked. Sulphur isotope ratios were determined at the CRPG (Nancy, France) using the technique described by Hu et al. (2003). Sulphide particles (0.5–1 mg) reacted with fluorine under a 25 W CO_2 infrared laser at 25–30 Torr in a vacuum chamber to produce SF_6, which was purified by dual gas chromatography. Multiple sulphur isotope ratios were measured with a Thermo Scientific MAT 253 mass spectrometer in dual inlet mode. Sulphur isotopes are expressed in delta notation ($\delta^{34}S$) relative to the international standard V-CDT based on the following equation:

$\delta^{34}S = [(^{34}S/^{32}S \text{ sample})/(^{34}S/^{32}S \quad \text{standard}) - 1] \times 1000$. The external precision on $\delta^{34}S$ was determined by multiple analyses of CDT material and internal reference materials (Maine and Alpha Aesar pyrite) and is better than 0.3‰ (2σ).

4.4. U-Pb dating of zircons

4.4.1. Mineral separation and sample preparation

Fresh hand specimens were disaggregated by electrical fragmentation using SelFrag at the John de Laeter Centre for Isotope Research. Approximately 1 kg of sample DC67 was loaded into a portable process vessel filled with de-ionized water. The base of the process vessel was fitted with a 410 μm mesh. As the samples was progressively disaggregated, grains and fragments smaller than 410 μm fell through the mesh and into a collection vessel that is isolated from further electrical pulses. Short pulses of high-voltage electrical fields were applied with a frequency of 2 Hz. Coarse fragmentation was achieved by applying five 140 kV pulses with an electrode gap of 40 mm. The voltage was stepped down to 130 kV for an electrode gap of 30 mm, and to 120 kV for an electrode gap of 20 mm. When the sample was disaggregated into fragments of 10 mm or less, a voltage of 100 kV was applied for approximately 450 pulses, at which point the entire sample had passed through the 410 μm mesh.

The heavy accessory minerals (including zircon) were concentrated using heavy liquids. Grains of zircon were hand-picked from heavy concentrate, and mounted in epoxy blocks. The grains were sectioned approximately in half and polished. Transmitted and reflected light photomicrographs and cathodoluminescence images were taken of select grains to document internal zircon structure and choose sites for analyses, avoiding cracks and inclusions.

4.4.2. U-Pb method

The U-Pb *in situ* age determinations were carried out on 6 polished zircons using Agilent 7700 quadrupole ICP-MS instruments, attached to a Photon Machines Excimer 193 nm laser system, at the GAU laboratory at the Department of Earth and Planetary Sciences, Macquarie University, Sydney, Australia. The analyses were carried out with a beam diameter of ca 40–50 μm with 5 Hz repetition rate and energy of around 0.06 μJ and 8 J/cm^2. The analytical procedures for the U–Pb dating have been described in detail previously (Jackson et al., 2004). A laser beam of 30 μm diameter with energies of 60–100 mJ/pulse and 5 Hz repetition rate was used for 100–120 s/analysis resulting in pits about 30 μm deep. Real-time data were processed using the GLITTER® software package. Age calibrations were checked using the GEMOC-GJ-1 with a TIMS age of 608.5 Ma (Jackson et al., 2004), TEMORA (Kemp et al., 2005) and the 91,500 international zircon standard (1064 Ma, Wiedenbeck et al., 1995). For the common-Pb correction we have employed procedure of Andersen (2002). Concordia diagrams (2σ error ellipses), concordia ages and upper intercept ages were calculated using the Isoplot/Ex software (Ludwig, 2003).

5. Results

5.1. HSE systematics

The new data for PGEs are summarized in Tables 2 and 3 and shown on Figs. 4 (Dergamysh) and 5 (Ivanovka), along with previous data for Au, Cu, Zn, Co and Ni after Melekestseva et al. (2013).

At Dergamysh, the Pd, Pt and Au concentrations in the 1-m core intervals reach 23 ppb (median = 4 ppb), 54 ppb (median < 5 ppb)

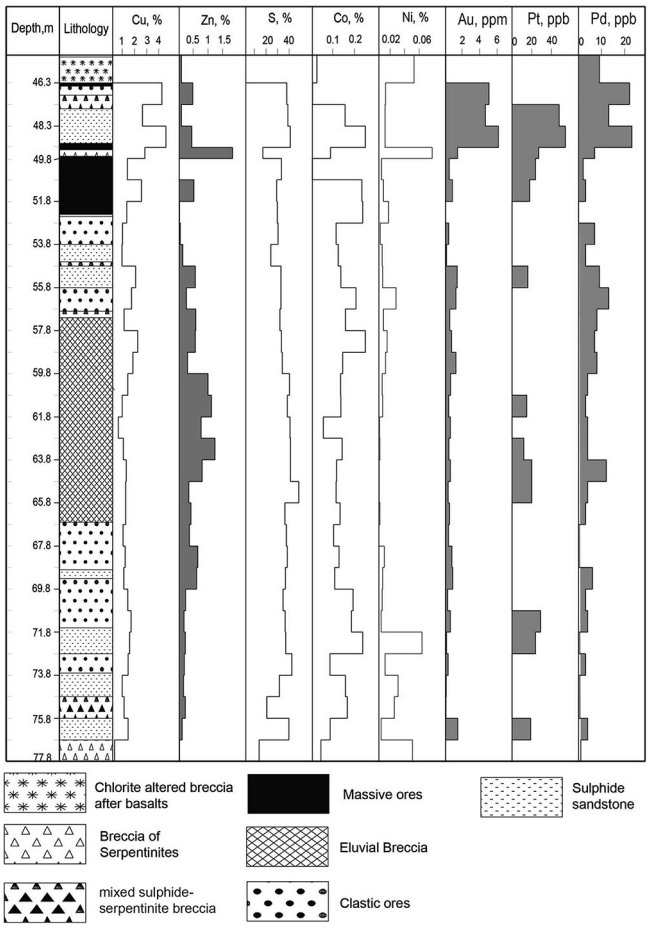

Fig. 4. Distribution of main (Cu, Zn, S) and trace (Co, Ni, Au, Pt, Pd) elements within the Dergamysh deposit drill core (adapted and integrated after Melekestseva et al., 2013).

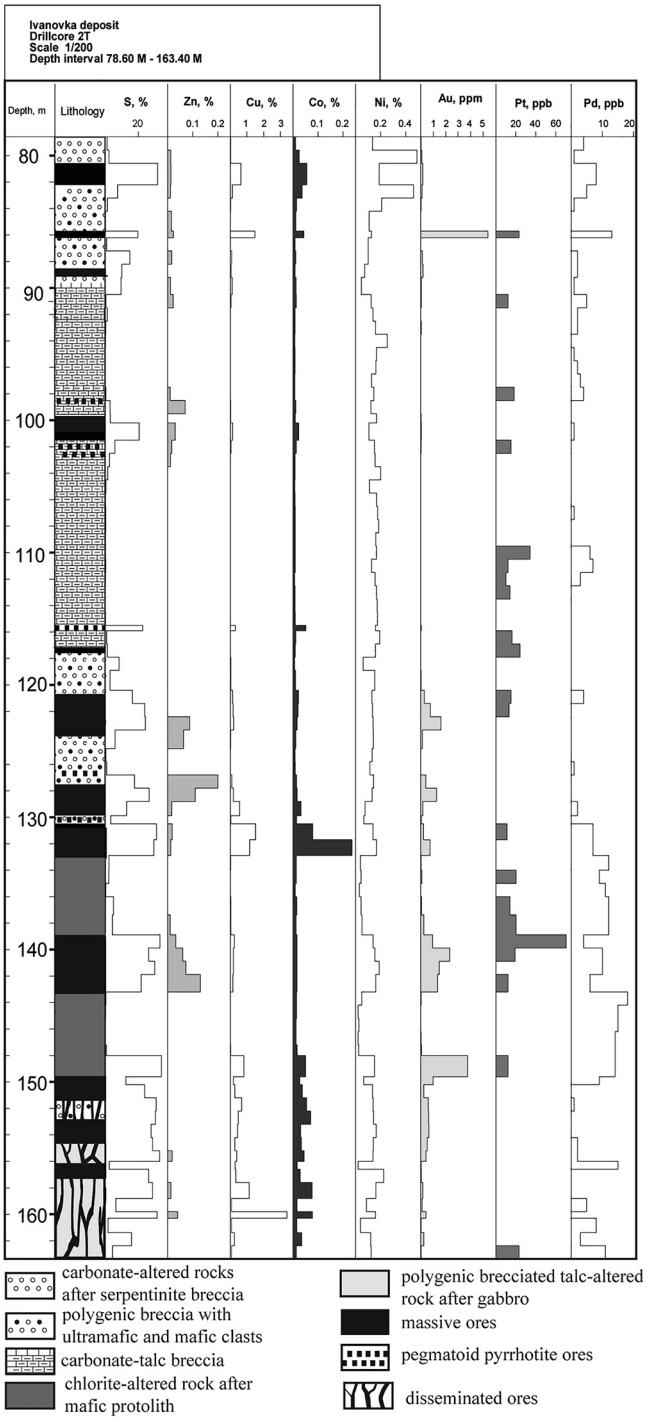

Fig. 5. Distribution of main (Cu, Zn) and trace (Co, Ni, Au, Pt, Pd) elements within the drill core across the Ivanovka deposit. Lithology of drill core is taken from Tesalina et al. (2003).

and 6170 ppb (median = 626 ppb), respectively. The maximum PGE, Au and Cu grades occur in the uppermost part of the deposit (Fig. 4). The samples with the highest Cu and Au contents also have the highest Pd and, with one exception, Pt contents (Table 2; Fig. 6), which suggests a statistical association between these elements (Table 6). The correlation coefficients calculated for Pt are decreasing in following order: Pt → Au → Cu → Pd (0.62 → 0.54 → 0.44 correspondingly). For Pd, the similar range has been calculated: Pd → Au → Cu → Pt (0.87 → 0.81 → 0.44 correspondingly).

The Re concentrations measured by Gannoun et al. (2003) in 6 sulphide sandstones (9–19 ppb) is lower than that in 11 sulphide breccias (12–42 ppb), whereas the Os contents (0.06–0.6 ppb) show no systematic difference between sulphide breccias and sulphide sandstones (Fig. 7). A positive correlation seems to exist between Os and Au (correlation coefficient Os_{com}/Au_{corr} = 0.80 for sulphide breccia), and between Re and Zn, whereas Re shows a negative correlation with Co (Fig. 8). Given the small number of samples analysed for all these elements (sulphide breccia n = 5), the statistical significance of these correlations remains limited.

At Ivanovka, the Pd, Pt and Au concentrations in the 1-m core intervals vary from below the detection limit to 18 ppb, 70 ppb and 5360 ppb, respectively. Their distribution along the drillhole is complicated by the very variable proportions of ore and host-rock components, as indicated by the variable measured S contents (Table 3). Overall, the Ivanovka sulphides are more enriched in Os (0.02–2.46 ppb) and less enriched in Re (0.18–6.10 ppb) relative to the Dergamysh sulphides (Gannoun et al., 2003).

The correlation coefficients (Table 7) and R^2-regression (Fig. 9) have been calculated separately for ores (massive, disseminated and pegmatoid pyrrhotite) and host rocks. In general, the correlation coefficients are not that significant when compared with the massive ores from the Dergamysh deposit (Table 6), with the maximum being attributed to Pd – Au (corr(Pd-Au) = 0.76; Table 7). Interestingly, correlation coefficients are sometime higher for the host rocks: e.g., corr(Cu-Pd) = 0.31 in host rocks is higher than that in ores (corr(Cu-Pd) = 0.22). The host rocks (mainly chlorite-altered mafic rocks) have slightly higher Pd contents than ores (Fig. 9B, D, and E). Two trends can be observed from the trace elements distribution plots: (a) low to high PGE at low Au – in rocks (no correlation) and (b) both PGE and Au are variable in ores (corr (Au-Pd) = 0.76, significant). Significant negative Ni-Pd correlation (−0.61) is observed in host rocks.

5.2. Sulphur isotopes

Sulphur isotopes for the Dergamysh ores (Table 5) show a range of $\delta^{34}S$ from −4.6 to 1.3‰, with a median value of −2.7‰ (n = 10). The sulphide breccias cover the entire observed $\delta^{34}S$ range, whereas the sulphide sandstones are characterised by less variable, negative $\delta^{34}S$ values, ranging from −3.9 to −2.1‰.

5.3. U-Pb dating of zircons

A total of 6 zircon grains were selected for analysis. Based on their morphology, we have distinguished two groups of zircon grains: (1) euhedral elongated bipyramidal prisms and (2) elongated or rounded grains. The former population is characterized by size ~250 μm and aspect ratio of ~1:3 (Fig. 10, grains DC67-06 and DC67-05). The second zircon type comprises xenomorphic grains with grain size of 100 to 200 μm (Fig. 10, remaining grains). The BSE images show that zircon grain DC67-01 has a sector-zoned inner core with dark thick rim (Fig. 10, DC67-01). The LA-ICPMS isotope data set is listed in Table 8 and plotted in a (Fig. 11). Ages younger than 1000 Ma are 204-corrected $^{206}Pb/^{238}U$ ages, whereas older ages are 204-corrected $^{207}Pb/^{206}Pb$ ages.

Eight analyses were performed, seven of which yield concordant ages ranging from 507 to 3312 Ma. One analyse was rejected due to high common-Pb and degree of discordance, with both attributes probably related to the extreme U-content (i.e. >1%; Table 8). Three analyses yielded Meso- and Paleo-Archean ages, three analyses yielded Paleo- and Neo-Proterozoic ages, and one analyses yielded a Cambrian age. All of them, however, are older than the Ordovician age of the rock. The Neoproterozoic age (636 ± 8 Ma) has been obtained on a zoned CL-light core overgrown by a dark Cambrian-age rim (507 ± 8; DC67-01R, Table 8).

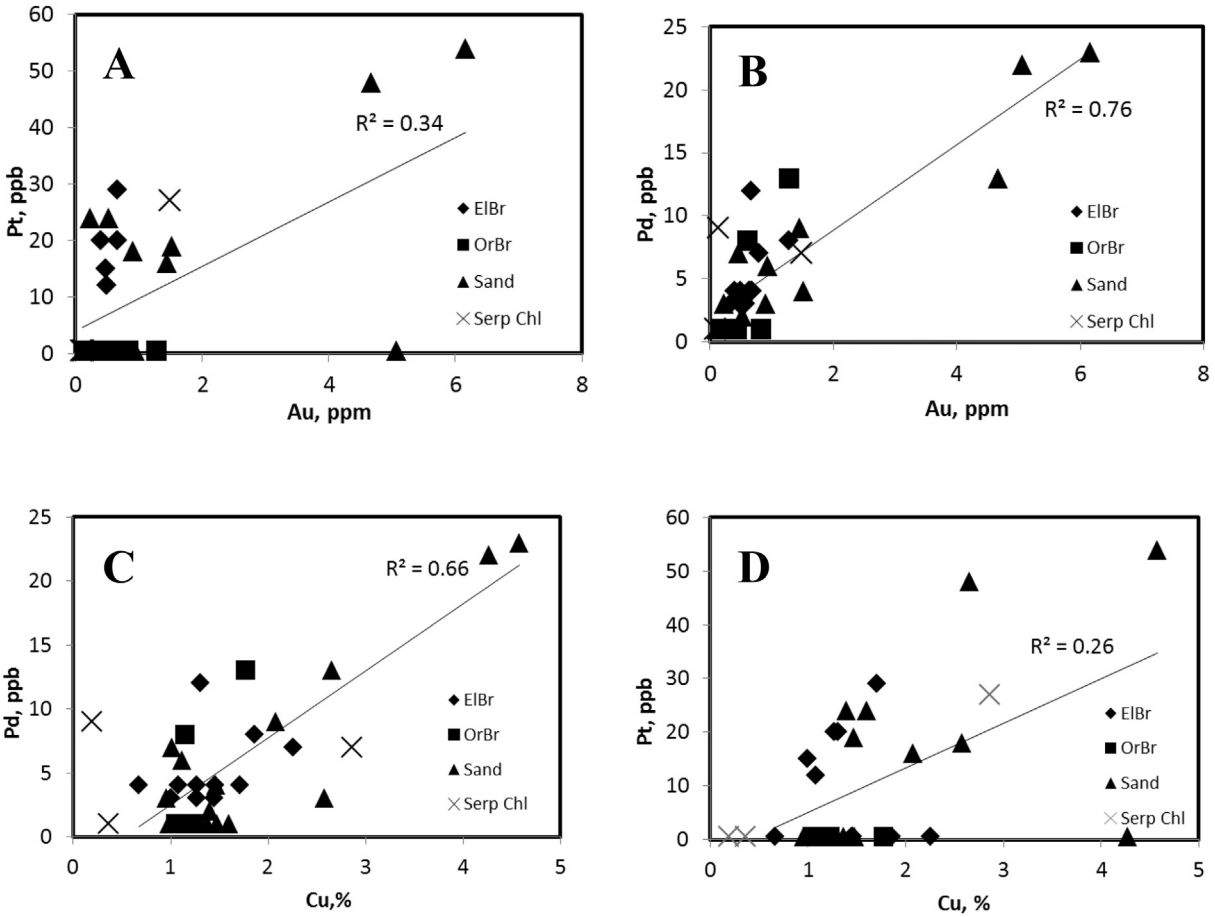

Fig. 6. Au vs Pt (A), Au vs Pd (B), Cu vs Pd (C), and Cu vs Pt (D) plots for the whole-ore intervals (Table 2) from drillcore 1T through the Dergamysh orebody. The linear regression line and R-squared values for massive sulphides are shown. Abbreviations for different lithology types are the same as in Table 2 (ElBr – eluvial sulphide breccia; OrBr – ore breccia; Sand – pyrite sandstone; Serp – serpentinite; Chl – chlorite-quartz altered basaltic breccia).

Table 6
Correlation coefficients between PGEs, Au and other metals for the Dergamysh deposit, inferred from the drillcore (1T, Fig. 1) intervals approximately 1 m long (Table 2). The correlation coefficients have been calculated for massive sulphides (S > 20%) for 30 ore intervals; ½ of detection limit was used for 'below detection limit' values. The correlation coefficients in the interval −0.30 to 0.30 are considered to be insignificant.

	Pt	Pd	Cu	Zn	Co	Ni	Au
Pt	1.00	0.44	0.54	−0.13	0.23	−0.03	0.62
Pd		1.00	0.81	0.08	0.02	−0.18	0.87
Cu			1.00	−0.07	0.19	0.07	0.89
Zn				1.00	−0.05	−0.26	−0.04
Co					1.00	0.43	−0.01
Ni						1.00	−0.06
Au							1.00

Two Paleoproterozoic ages were obtained on a zoned prismatic crystal (DC67-05) and an elongated homogeneous dark zircon grain (DC67-04). Paleoarchean (3312 ± 46 Ma) and Mesoarchean (3154 ± 46 Ma) ages were obtained on different parts of the same zircon grain (DC67-02). Another Mesoarchean age of 3106 ± 24 Ma was obtained on a homogeneous dark elongated zircon grain (DC67-03, Table 8).

6. Discussion and model of hydrothermal systems formation

6.1. Highly Siderophile Elements abundance and distribution

The median Pt and Pd contents of the Dergamysh and Ivanovka deposits are lower than those from other Urals VHMS deposits hosted by island-arc mafic to felsic volcanics (Table 1; Fig. 12). The median Pd/Pt ratios are however comparable only with those in the most Pt-rich Urals-type VHMS deposits, such as Gai, Levikha group and Blyava (Table 1; Fig. 12). As a result, in a Pt vs Pd/Pt diagram, the studied deposits plot off the trend described by other Urals VHMS deposits (Fig. 12). Modern mafic- and ultramafic-hosted VHMS deposits from the Mid-Atlantic Ridge (Pašava et al., 2007) also have higher Pd values (averaging 32 ppb for Turtle Pits and 124 ppb for the Logatchev field). The low Pd/Pt ratios of the Dergamysh and Ivanovka deposits are dissimilar to those in average MORB basalts, but comparable to those in mantle peridotite xenoliths in island-arc volcanic rocks (Fig. 13; Kepezhinskas and Defant, 2001), suggesting a possible supra-subduction mantle source of the PGEs.

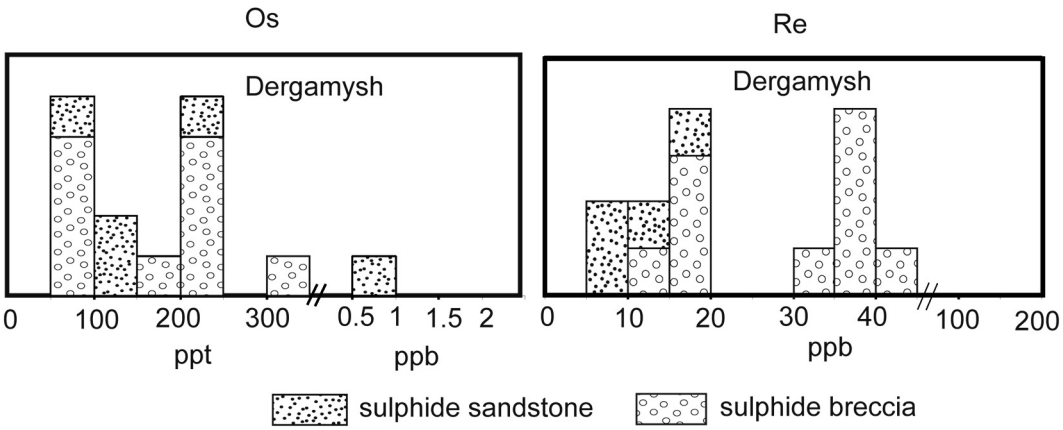

Fig. 7. Re and Os distribution in different ore facies of the Dergamysh hydrothermal system (data from Gannoun et al., 2003).

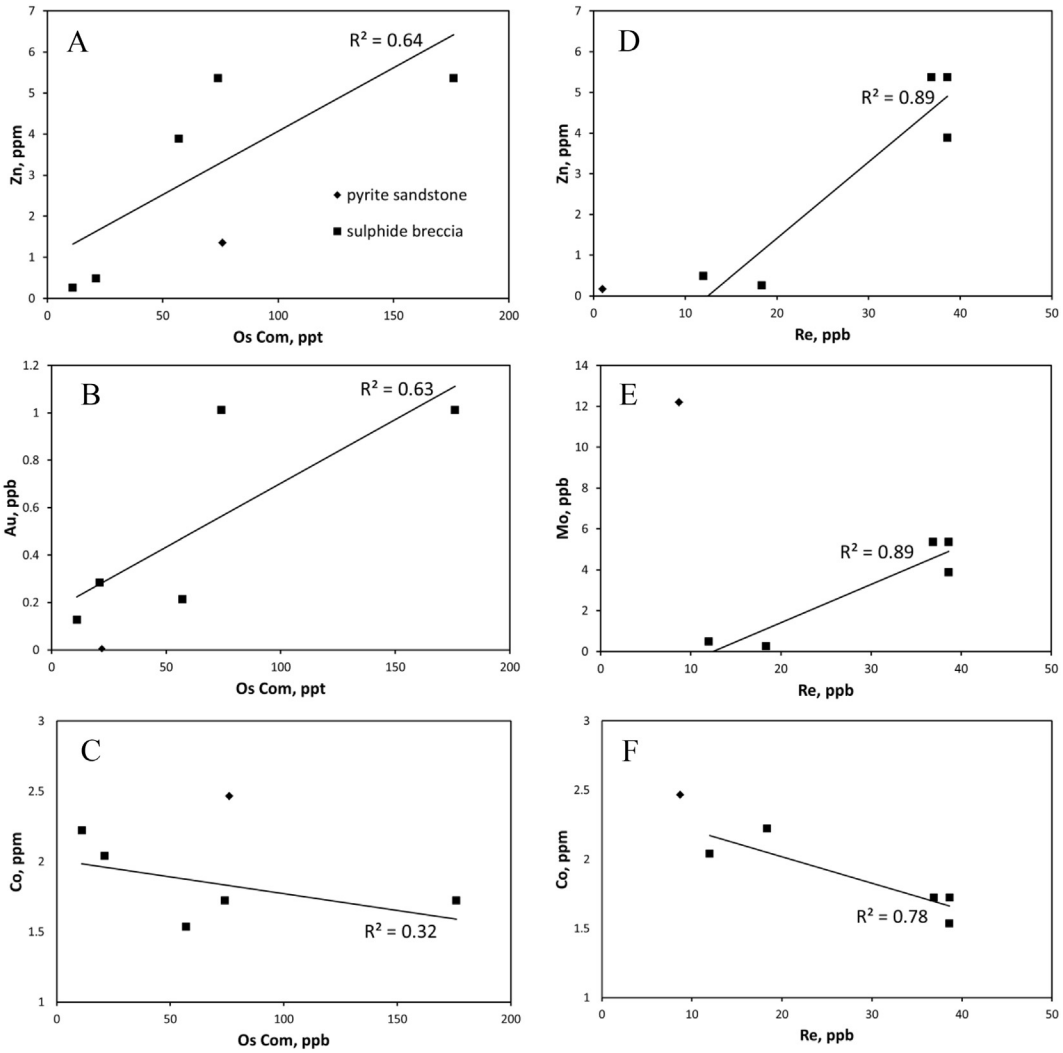

Fig. 8. Common Os and Re versus Zn, Au, Co and Mo for sulphide breccias and sandstone from the Dergamysh deposit (Table 4). R-squared value (R^2) is displayed for sulphide breccia. Note that the limited number of variables (n = 5) does not allow precise estimation of correlation coefficient.

The positive correlations of Au and Cu with Pd and, in part, Pt in the Dergamysh drillhole samples (Fig. 6), suggest that the PGEs are mostly concentrated in chalcopyrite-rich assemblages and may thus belong to a high-temperature sulphide facies. Melekestseva et al. (2013) recognised the presence of minor Au peaks along the drillhole, which correspond to the tops of fining-upward rhythmic units made of sulphide breccias and sandstones, and ascribed them to hydrothermal zone-refining or to submarine supergene enrichment. Corresponding peaks are also observed in the Pd profile (cf. intervals 58.8–59.8, 68.8–69.8), but are not clearly visible in

Table 7
Correlation coefficients between PGEs, Au and other metals for the Ivanovka deposit, separately for ores (massive, disseminated and pegmatoid pyrrhotite) and host rocks (in *italic*). The samples studied come from the drillhole intervals approximately 1 m long (Table 3). ½ values have been taken for 'below detection limit' analysis. The correlation coefficients in the interval -0.30 to 0.30 are considered to be insignificant.

	Pt	Pd	Cu	Zn	Co	Ni	Au
Pt	1.00	−0.25	0.00	0.03	−0.11	0.08	0.30
Pd	*0.10*	1.00	0.22	0.02	0.22	0.18	0.76
Cu	*−0.06*	*0.31*	1.00	−0.07	0.55	0.26	0.24
Zn	*−0.04*	*−0.15*	*0.04*	1.00	−0.19	0.19	0.15
Co	*−0.08*	*0.31*	*0.53*	*0.11*	1.00	0.31	0.05
Ni	*−0.05*	*−0.61*	*−0.02*	*0.09*	*0.40*	1.00	0.15
Au	*0.17*	*0.28*	*0.26*	*0.11*	*0.52*	*0.06*	1.00

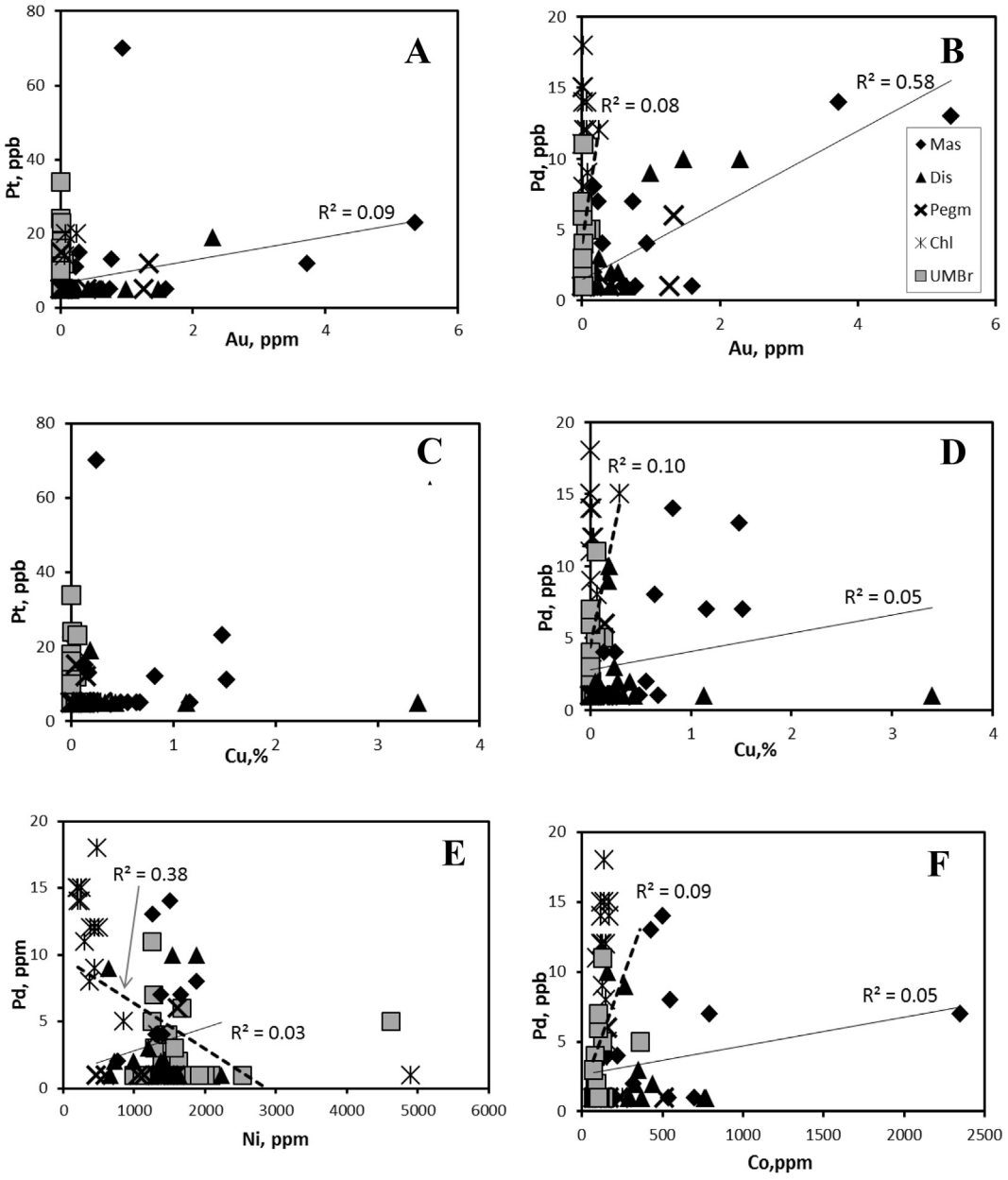

Fig. 9. Au vs Pt (A), Au vs Pd (B), Cu vs Pt (C), Cu vs Pd (D), Ni vs Pd and Co vs Pd (F) plots for the mineralised sequence of the Ivanovka deposit (Table 3) from drillcore 2T (Fig. 3). The linear regression line and R-squared values are shown separately for ores (solid line; massive [Mas], disseminated [Dis] and pegmatoid pyrrhotite [Pegm]) and host rocks (dashed line; chlorite-altered rocks after mafic photolith [Chl] and polygenic altered breccia with ultramafic and mafic clasts [UMBr]).

the Pt profile (Fig. 4). The similar positive correlation exist for the Ivanovka deposit (corr(Au-Pd) = 0.71; Fig. 9B), other correlations are less significant compared to those for massive Dergamysh ores.

Rhenium abundances in the Dergamysh (1–41 ppb; Fig. 7) and Ivanovka (1–6 ppb) deposits (data from Gannoun et al., 2003) are comparable with those in other Urals VHMS deposits

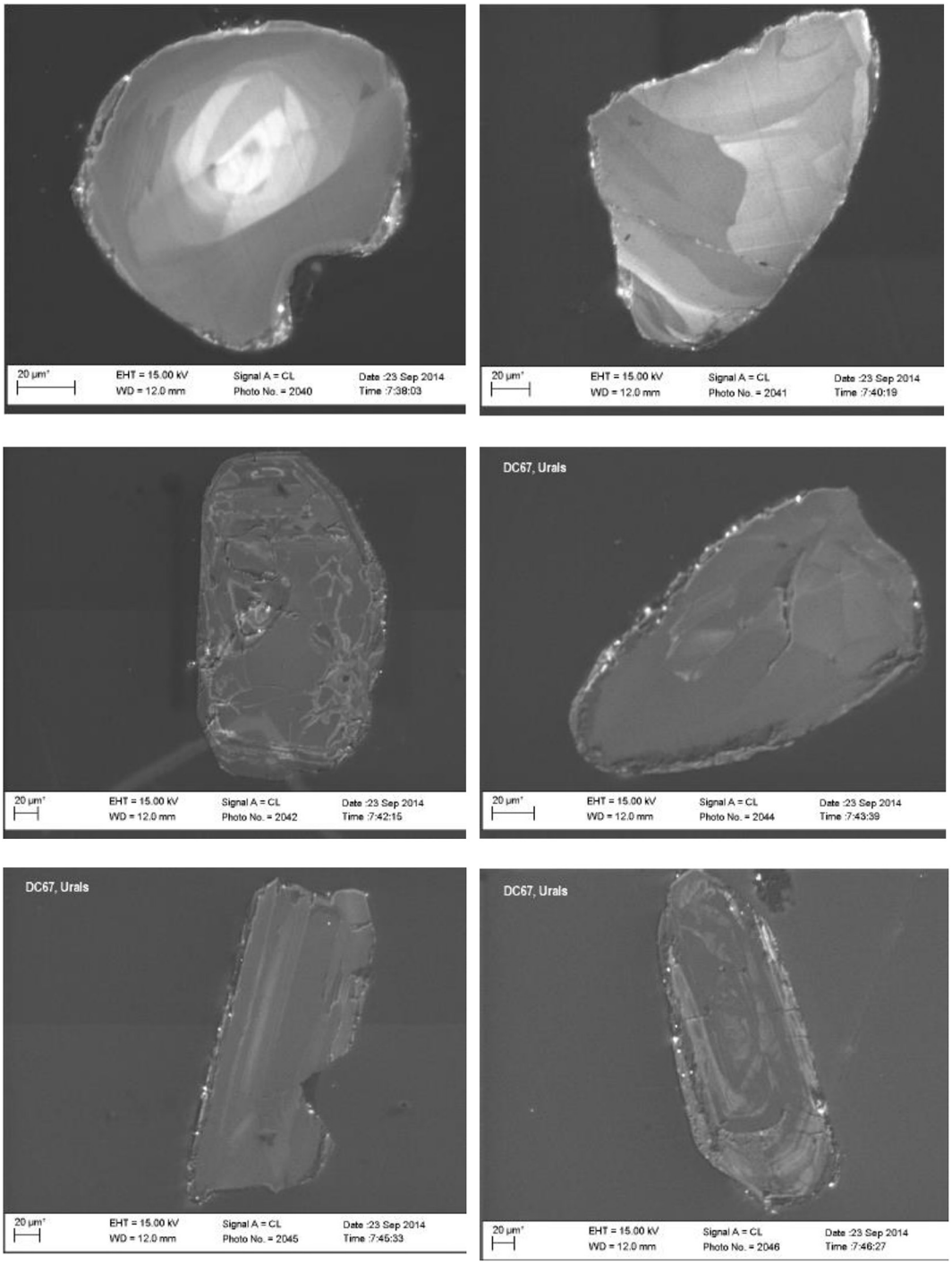

Fig. 10. Catodoluminescence images of studied zircon grains from the Dergamysh deposit.

(e.g., Tessalina et al., 2008b, 2017) and in some of the VHMS deposits in the Iberian Pyrite Belt (Mathur et al., 1999). Modern TAG sulphides also exhibit similar Re concentrations, ranging from 0.1 to 72 ppb (Brügmann et al., 1998; Ravizza et al., 1996). Rhenium contents tend to be lower in the sulphide sandstones compared with the sulphide breccias (Fig. 7), which may reflect enhanced Re loss by seafloor weathering of the finer-grained sulphides. However, the positive correlation of Re vs. Zn and the negative correlation of Re vs. Co (Fig. 8) would suggest a higher affinity of Re with low-temperature polymetallic assemblages, which is also supported by the low Re contents in chalcopyrite-rich outer zones of seafloor hydrothermal chimneys from Yaman-Kasy deposit (Tessalina et al., 2017).

Chondrite-normalized HSEs pattern for the Dergamysh deposit ores is similar to other Urals and modern mafic-ultramafic hosted VHMS deposits (with the exception of lower Pd), and is about one to three orders of magnitude higher than those in the host-rocks (Fig. 13), as expected from the high affinity of HSEs for S. A higher HSEs enrichment in the ores relative to their host-rocks can be explained by high sulphide/fluid partition coefficients (not known) and high fluid/sulphide ratios, e.g. when enduring circulation of fluids allows continuous incorporation of HSEs within the

Table 8
Isotopic ages (Ma), U-Th concentrations and corrected isotopic ratios for zircons from sample DC67. The errors are reported as 1σ for corrected isotopic ratios and as 2σ for U-Pb ages.

	Conc (ppm)		Corrected ratios					U-Pb ages (common-Pb corrected)			
ID	U	Th	Pb^{207}/Pb^{206}	Pb^{207}/U^{235}	Pb^{206}/U^{238}	Pb^{208}/Th^{232}	U^{238}/Th^{232}	Pb^{207}/Pb^{206}	Pb^{207}/U^{235}	Pb^{206}/U^{238}	Pb^{208}/Th^{232}
01C	368	110	0.0652 ± 9	0.93 ± 1	0.1037 ± 8	0.0251 ± 6	3.37 ± 21	784 ± 66	669 ± 14	636 ± 8	501 ± 22
01R	207	141	0.059 ± 1	0.66 ± 1	0.0818 ± 7	0.0214 ± 5	1.48 ± 9	564 ± 88	517 ± 16	507 ± 8	428 ± 20
02L	59	34	0.245 ± 4	21.6 ± 3	0.6393 ± 52	0.1608 ± 42	1.76 ± 11	3154 ± 46	3166 ± 26	3186 ± 40	3013 ± 148
02D	133	48	0.271 ± 4	25.4 ± 4	0.6787 ± 55	0.1427 ± 40	2.78 ± 17	3312 ± 46	3322 ± 26	3339 ± 42	2695 ± 140
03	410	299	0.238 ± 2	20.0 ± 2	0.6086 ± 34	0.1385 ± 17	1.38 ± 9	3106 ± 24	3089 ± 14	3064 ± 26	2622 ± 60
04	652	683	0.133 ± 1	7.17 ± 7	0.3921 ± 20	0.0898 ± 16	0.96 ± 6	2132 ± 36	2132 ± 18	2132 ± 22	1738 ± 58
05	389	428	0.136 ± 11	7.30 ± 5	0.3895 ± 21	0.1060 ± 13	0.91 ± 6	2176 ± 28	2149 ± 14	2121 ± 20	2036 ± 48
06#	12,465	777	0.128 ± 11	1.63 ± 1	0.0928 ± 13	0.0264 ± 124	16.15 ± 1.01	2063 ± 326	982 ± 112	572 ± 14	527 ± 488

All data corrected for common Pb. # – rejected analysis (high U content). Abbreviations: C – grain core zone; R – grain rim zone; L – light part; D – dark part.

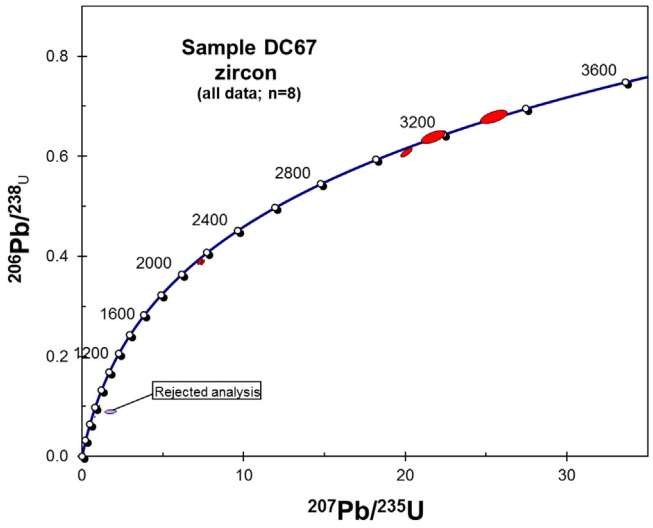

Fig. 11. Concordia diagram for LA-ICPMS data for zircons from Dergamysh host-rocks.

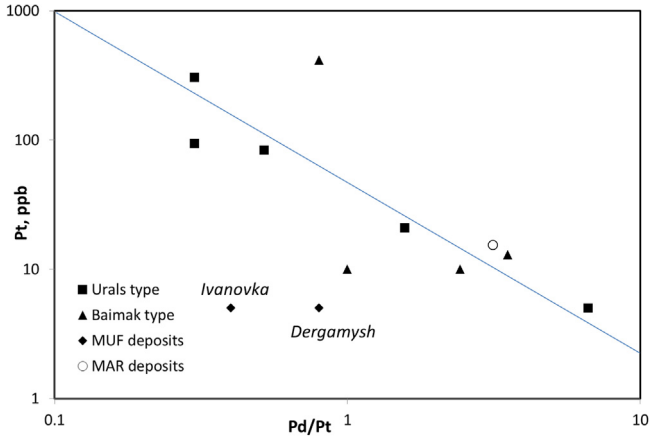

Fig. 12. Pt-Pd distribution within Urals VHMS deposits (average values are used for literature data, and median values for Dergamysh and Ivanovka deposit in this study). Data for Urals deposits after Volchenko et al. (1993), Dobrovolskaya and Distler (1998), and this study (Table 1). Data for modern Mid-Atlantic Ridge (MAR) deposits after Pasava et al. (2007) and Cave et al. (2003). Urals-type deposits are hosted by bimodal volcanic series. Baimak (Kuroko)-type deposits are hosted by felsic rocks (see Table 1).

precipitated sulphides. A similar high HSEs enrichment has been reported for modern sulphides from the Turtle Pits, Logatchev and Rainbow hydrothermal fields from Mid-Atlantic Ridge (Fig. 13; Pašava et al., 2007; Cave et al., 2003).

6.2. U-Pb dating of Dergamysh host rocks

The U-Pb ages obtained for zircons from the Dergamysh ore-hosting rocks range from Archean (3.3–3.1 Ga) to Cambrian (507 Ma). This result is rather unexpected given that the MUF serpentinitic melange mainly contains fragments of arc-derived Ordovician to Carboniferous igneous and sedimentary rocks.

The Archean to Proterozoic ages in our study may be related to the old continental crust fragments present in the basement of the intra-oceanic arc, a scenario that has recently been shown in modern intra-oceanic arcs of Vanuatu (Buys et al., 2014) and the Solomon Islands (Tapster et al., 2014). The remnants of older crustal fragments in these two settings have been demonstrated by the presence of old Archean zircons. Archean and Proterozoic zircons have also been extracted from Urals peridotites (e.g., dunites within a number of dunite-clinopyroxenite massifs), with U-Pb ages ranging from Neoarchaean (2781 ± 56 Ma), Paleoproterozoic (2487 ± 33 Ma and 1881 ± 9 Ma), Mesoproterozoic (1172 ± 9.8 Ma) to Mid-Paleozoic (414.8 ± 3.9 – 473 ± 3.7 Ma), reflecting the multi-stage formation history of the Uralian Platinum Belt (Malitch et al., 2009; Fershtater et al., 2009).

The U-Pb zircon ages from Dergamiysh deposit are comparable to that of detrital zircons from sandstones in the adjacent Bashkir Anticlinorium of the Southern Urals (Lemeza Subformation of the Karatavian Zil'merdak Formation, standard of the Upper Riphean in northern Eurasia). This anticlinorium borders the East European Platform and MUF (Fig. 1). For these sediment, two distinct detrital zircons populations have been established: Paleoproterozoic (1.8–2.1 Ga) and Archean (2.3–3.1 Ga) (Romanyuk et al., 2013). These Paleoproterozoic ages are correlated with episode of the Archean protocratons assembling (Sarmatia, Volga-Uralia, Kola, Karelia) to form Proto-Baltica. By analogy with sandstone, the zircons in our study could be originated from the eroded basement of the East European Platform, mostly of its Volga-Uralian part (Romanyuk et al., 2013), which has been formed as a result of the Neoarchean plume event at 2.74–2.6 Ga, transforming earlier Archaean continental crust (3.4–3.0 Ga) (Mints, 2011).

The similarity of U-Pb zircon ages from Dergamysh ore-hosting rocks with the age of adjacent Archean continent, together with the presence of old Archean zircons within Urals peridotites, support the possibility of old continental crust fragments being present in the base of the Uralian island arc.

6.3. Sulphur sources and stable isotopes fractionation processes

The $\delta^{34}S$ values for the Dergamysh samples ($-4.6‰ < \delta^{34}S < +1.3‰$; Table 5) are rather low compared to the $\delta^{34}S$ values for most modern seafloor hydrothermal deposits, which cluster in a range from +1 to +5‰ (e.g., Shanks, 2001), and similar to that from other mafic-hosted (Cyprus-type) Urals VHMS deposits (−3.4 to

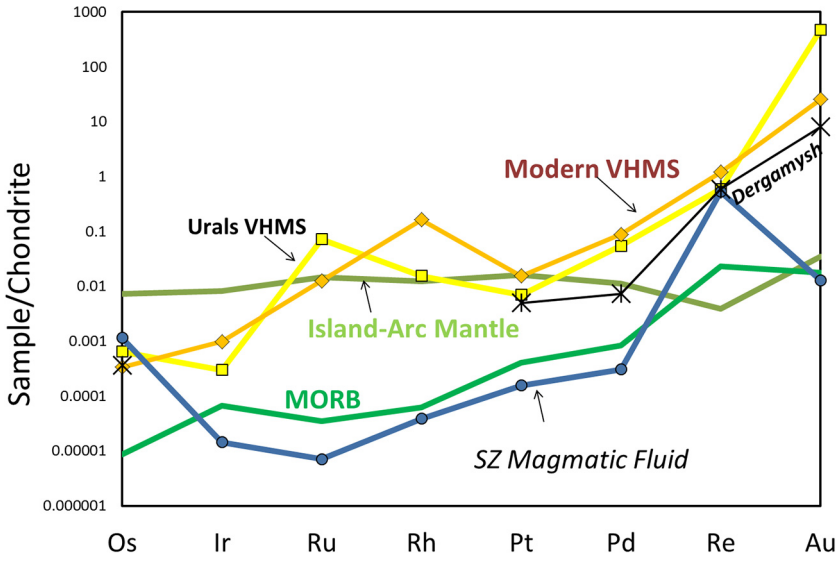

Fig. 13. Chondrite-normalized HSE (PGE-Re-Au) patterns for Dergamysh deposit from this study (Ir, Ru, Rh are missing). Average abundances for Urals VHMS deposits (see Table 1 for data sources), modern mafic-ultramafic hosted VHMS deposits from the MAR (Pašava et al., 2007; Cave et al., 2003), global MORB (Crocket 2002), island-arc mantle peridotite (Kepezhinskas and Defant, 2001), and supra-subduction zone (SZ) magmatic fluid (Tessalina et al., 2008; Yudovskaya et al., 2008) are shown for comparison. Chondrite data after McDonough and Sun (1995).

+4.3‰; n = 3; Prokin and Buslaev, 1999). There is a systematic shift towards negative values (by about 2–3‰) in the sulphide sandstone relative to the massive ores, a feature that was also observed in the Alexandrinka Baimak-type deposit, hosted by bimodal volcanics (author's unpublished data). By analogy with modern seafloor basaltic and peridotite-hosted hydrothermal systems, the sulphur in Devonian hydrothermal deposits may have two main sources: seawater sulphate (+19‰ < δ^{34}S < +28‰, Kampschulte and Strauss, 2004) and mantle sulphides with a δ^{34}S value being estimated at +0.1 ± 0.5 (e.g., Shanks, 2003), or more recently at −1.3‰ (Labidi et al., 2013). The negative δ^{34}S anomaly observed in the Dergamysh ore sulphides requires a source for isotopic fractionation of sulphur, which cannot be explained by the simple mixing of surrounding rock and seawater (e.g., Shanks, 2001; Kim et al., 2004). Other possibilities include fractionation of stable S isotopes due to phase separation (boiling), and biogenic processes.

Sulphur isotope fractionation can occur during boiling of hydrothermal fluids leading to the phase separation (e.g., McKibben and Eldridge, 1990), because H_2 loss during the boiling of hydrothermal fluid takes a much shorter time than H_2S loss, the composition of the remaining fluid evolves to a more oxidized state (e.g., Drummond and Ohmoto, 1985). Such a change would lead to preferential oxidation of $H_2^{34}S$ into sulphate. The boiling and oxidation of the H_2S model might explain the observed low δ^{34}S values of Dergamysh ores because the δ^{34}S values of sulphates and sulphides decrease as the oxidation progresses. Significant boiling in the hydrothermal system is required for sulphur isotopic fractionation by this model. Phase separation of hydrothermal fluid by boiling hasn't been reported for Dergamysh or other mafic-ultramafic deposits in Urals. However, this process was reported for modern seafloor hydrothermal systems situated at the East Pacific Rise, the Juan de Fuca ridge, and the Mid Atlantic ridge (Seyfried and Ding, 1995). However, the sulphur isotopic fractionation in chimney sulphides wasn't detected at those hydrothermal sites. This implies that the oxidation of H_2S is not a major controlling factor of the sulphur isotope composition of a hydrothermal chimney (Kim et al., 2004), possibly because the seafloor hydrothermal systems are not closed systems and equilibrium is not reached in sulphur isotopic fractionation by oxidation of H_2S. In the other hand, if the S fractionation associated with boiling would affect the studied sulphides, it would be potentially even more pronounced in fragments of massive sulphide ores preserved in ore breccia, which is not a case in our study. Therefore phase separation, if it occurs, cannot be the controlling factor for the sulphur isotope composition of Dergamysh ores in our study.

Sulphide produced by bacterial reduction is enriched in light ^{32}S (Ohmoto, 1986). Fractionation of sulphur isotopes during bacterial reduction in a hydrothermal system typically produces sulphide phases with δ^{34}S values of −40‰ to −10‰ (Ohmoto, 1986; Brunner and Bernasconi, 2005). Remobilised biogenic sulphur in sediments is one of the main reservoirs related to seafloor hydrothermal systems, but its influence on the sulphur composition of hydrothermal ore deposits is limited to sediment hosted ridge systems, such as the Guaymas Basin (Peter and Shanks, 1992), the Escanaba Trough (Zierenberg et al., 1993), and the Middle Valley (Goodfellow and Blaise, 1988). The sediment layer is poorly developed at both Dergamysh and Ivanovka sites, which is indicative of the small influence exerted by isotopically light sulphide of biogenic origin from the sediments, but other sources can't be excluded.

Many organisms near vent sites derive their metabolic energy from the utilisation of sulphur. Among the metabolic processes that utilize sulphur, the reduction of sulphate to sulphide produces a significant isotope effect (Kennicutt et al., 1992). In a case of mafic-ultramafic hosted modern hydrothermal sites, sulphide oxidisers belonging to the *Thiomicrospira* species and the epsilon-proteobacteria *Sulfurovum lithotrophicum* were identified in the carbonate chimneys and the hydrothermal fluids of the LCHF (Brazelton et al., 2006). Moreover, sulphur-cycling bacteria *Thermococcales* and *Crenarchaeota* are inferred to be present in the subsurface (Brazelton et al., 2006). Elemental sulphur is a product of sulphide oxidation and is present in some extent in serpentinite (Delacour et al., 2008), leading to light δ^{34}S values of ca. −5.5‰, indicating the microbial sulphide oxidation with concomitant formation of sulphate.

The low δ^{34}S values in a range from to −5 to −30‰ were reported for sulphides and sulphates from modern seafloor mafic and ultramafic hosted hydrothermal systems such as the Hess Deep in the eastern Pacific, the Iberian Margin (Alt and Shanks, 1998), and the Lost City (Delacour et al., 2008). Such low values

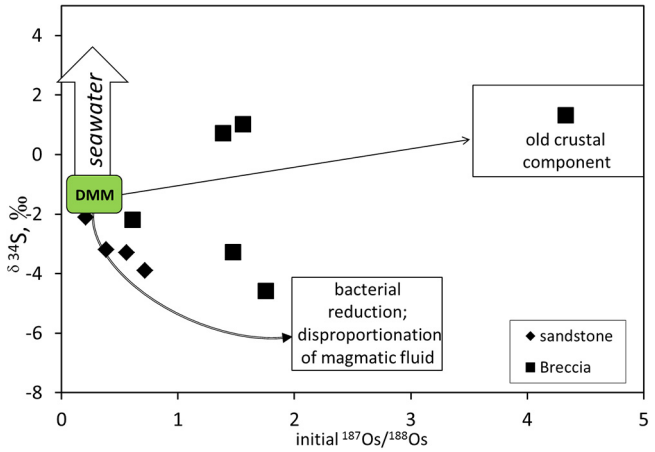

Fig. 14. Initial $^{187}Os/^{188}Os$ ratios versus $\delta^{34}S$ values for sulphides (breccia and sandstone) from the Dergamysh deposit. See text for end-members composition. Abbreviations: DMM – depleted mantle, SZ – subduction zone.

were attributed to sulphate reduction by thermophilic or hyperthermophilic micro-organisms that survive chemo-synthetically on the abundant H_2 or CH_4 that is generated during serpentinisation (Alt and Shanks, 1998; Delacour et al., 2008). In Degamysh deposit ores (Table 5; Fig. 14), the sulphide sandstones show the lowest $\delta^{34}S$ values, suggesting a contribution of isotopically light sulphur. This lighter sulphur may arise from a number of different processes, including bacterial reduction, similar to those described for the serpentinite-hosted sulphides from the Hess Deep in the eastern Pacific and from the Iberian margin (Alt and Shanks, 1998). Such fractionation, coupled with Rayleigh distillation processes, may well explain the $\delta^{34}S$ data in the Dergamysh deposit, whose original substrate was most likely made of serpentinised ultramafic and chloritised mafic rocks (cf. Melekestseva et al., 2013).

However, it can be also attributed to kinetic processes leading to redeposition of pyrite around pyrite clasts, as it is a case for other Urals VHMS deposits (author unpublished data), where the pyrite margins are enriched in lighter ^{32}S isotope compare to pyrite clasts in the order of 2‰.

6.4. Sources of metals and sulphur using Os-Pb-S systematics

The combined Pb-Os-S isotope systematics can be used to identify the sources involved during metals and sulphur mobilisation. For example, the Os isotopic composition in modern hydrothermally active TAG mound (Mid-Atlantic Ridge) is controlled by the extent to which the hydrothermal fluid has mixed with seawater (Brügmann et al., 1998). The Os isotopic composition of the TAG hydrothermal fluids reflects that of the basalt substrate ($^{187}Os/^{188}Os$ ~0.12) and is significantly different from that of the metalliferous sediments, which have the same isotopic signature as modern seawater ($^{187}Os/^{188}Os$ ~1.047). More recent study suggest that the $^{187}Os/^{188}Os$ isotopic compositions of massive sulphide from a large number of modern hydrothermal fields (East Pacific Rise, Mid-Atlantic Ridge, Central Indian Ridge, South West Indian Ridge and Back-Arc Basin) yield a narrow range (1.004–1.209), which is explained as a seawater-derived component, suggesting that the initial $^{187}Os/^{188}Os$ isotope compositions of ancient seafloor hydrothermal sulphide deposits are possible for analysing ancient seawater Os components (Zeng et al., 2014)

The isotopic composition of lead from deposits and host rocks of the Mid-Atlantic ridge is remarkably homogeneous and corresponds to the host MORB (Mid-Ocean Ridge Basalts). In contrast, the isotopic composition of lead in massive sulphides and rocks from island arcs varies more widely as is the case for the Mesozoic Japanese island arc (Tatsumoto, 1969) and the Tertiary Macuchi island arc (Chiaradia and Fontboté, 2001). This has been explained in terms of a variable contribution of lead from the subducted oceanic crust and sediments into the ore-forming fluids. Another potential source of lead in intra-oceanic island arc constitutes the cryptic relics of continental crust which can be rifted and dragged far from original continent within the basement of arcs, as it is the case in modern intra-oceanic arc Vanuatu (Buys et al., 2014) and the Solomon island arc (Tapster et al., 2014).

Several components (slab, oceanic crust, possible fragment of continental crust) are involved in geotectonic evolution of subduction zones and may contribute into isotopic and elemental balance. Island arc magmatism generated above a subducted oceanic plate is derived both from the slab and from the overlying mantle wedge. High-pressure dehydration of subducted crust releases fluids that act as a flux for the melting of mantle wedge peridotites and generation of arc magmas (e.g., Hofmann, 1997). Dehydration of the subducted slab releases water-rich fluids enriched in volatile phases and some metals into the overlying mantle wedge, inducing its partial melting. The produced silicate magma contains significant amount of water and volatile phases. When the solubility of the multicomponent volatiles in the silicate melt is exceeded, they are exsolved from the silicate melt as a separate fluid phase (e.g., Halter and Webster, 2004). This magmatic fluid is enriched in sulphur, chlorine, fluorine, alkalis, and chalcophile metals.

By analogy with the modern hydrothermal systems, the possible end-members (metal/sulphur sources) which may contribute to the Dergamysh and Ivanovka deposit ores, can be identified as: hydrothermal fluid (which contains the metals released from the mafic-ultramafic substrate rocks); Devonian seawater; possible contributions from magmatic and/or slab-derived SSZ fluids. In order to estimate the proportions of metals and sulphur contribution from these components, one needs an estimate of the isotopic compositions of these end-members.

6.4.1. Devonian seawater composition

The Os isotopic composition of Devonian seawater is inferred to be close to that of metalliferous and organic-rich sediments (Ravizza et al., 1996), approaching 0.2 for metalliferous sediments from other Urals hydrothermal systems (Tessalina et al., 2008b). The latter value is slightly less radiogenic than that estimated at *ca.* 0.45 for the Devonian seawater at Frasnian-Fammenian boundary (372 ± 4 Ma) by Turgeon et al. (2007). Although these values should be treated with caution because of the short residence time of Os in seawater (ca. 40 kyr).

The S isotopic composition of Devonian seawater is in a range from 19 to 28‰, inferred from the structurally substituted sulphate in carbonate and marine evaporitic sulphate by Kampschulte and Strauss (2004).

6.4.2. Magmatic fluid

The presence of magmatic aqueous-carbonic fluid with significant contents of H_2S has been detected in some of the Urals VHMS deposits (e.g., Bailly et al., 1999). This fluid is typically associated with felsic magmas and capable to carry significant amounts of metals. For comparison, the Os contents of magmatic fluids from modern volcanoes (e.g., Yudovskaya et al., 2008) exceed the modern hydrothermal fluid contents (e.g., Sharma et al., 2000) by 4 orders of magnitude. It is evident that even tiny amounts of this metals-rich magmatic fluid will influence the Os-Pb budgets in the magmatic-hydrothermal system, with isotopic composition similar to that of mafic magmas, possibly derived from depleted metasomatised mantle.

The input of magmatic volatiles into the hydrothermal system may be dominated by light sulphur, as it was proposed for the modern system in the Lau Basin by Herzig et al. (1998). This process is represented by the disproportionation of magmatic SO_2 gas ($\delta^{34}S \sim 0‰$) being divided into sulphide (enriched in ^{32}S) and sulphate (depleted in ^{32}S; Ohmoto and Lasaga, 1982). Possible magmatic contribution into the Urals hydrothermal systems have been reported by Karpukhina et al. (2013) and Bailly et al. (1999) for deposits hosted by bimodal sequences, based on melt inclusions and fluid inclusions studies. High concentrations of ore-forming metals such as Cu, Zn, Se and Au in magmatic fluid and melt which are trapped in the phenocrysts and glass of the volcanic rocks of the Uzelginsk ore field were proposed as direct evidence of magmatic contribution to hydrothermal deposits (Karpukhina et al., 2013).

However, this metal-rich magmatic fluids generally released from volatile-rich felsic magmas, which are prevalent at convergent margins setting (e.g., Huston et al., 2011). In suture zone setting, the mafic composition of magmas prevails, which may limit the extent of magmatic fluid contribution into hydrothermal systems.

6.4.3. Subduction-related fluid

In a case of Urals, subduction-related fluid may inherit the isotopic composition of Proterozoic rocks, which have entered into subduction zone and caused high-pressure metamorphism accompanied by release of fluid. This fluid provoked hydrous melting in the overlying mantle wedge and can be traced by its lead isotopic composition. Lead isotope data can provide a useful tool for evaluating the influence of a subducting component on the compositions of hydrothermal systems. The Pb isotopic composition of Proterozoic rocks is characterised by low model μ-values. In fore-arc setting, the model μ-values of Urals VHMS deposits is close to that of Proterozoic rocks (Tessalina et al., 2016a). In MUF zone and back-arc settings, the anhydrous decompressional melting of oceanic crust prevails, with the highest μ-values corresponding to that of Ordovician crust (~9.6), with nil contribution from subduction-related fluid.

The contribution from subduction-related fluid is not further supported by relatively low $\delta^{34}S$ values of sulphides from Dergamysh deposit. In a case of forearc fluids contribution, one would expect high-$\delta^{34}S$ values, as observed in retrograde pyrite from high-*P* terrains that are dominated by meta-igneous and mantle-derived rocks (Marschall and Shimizu, 2012).

6.4.4. Host rocks sourced by hydrothermal fluid

Dergamysh and Ivanovka deposits are hosted by mantle-derived mafic-ultramafic rocks, possibly originated from metasomatised depleted mantle in supra-subduction zone setting.

Lead isotopic compositions of mafic-ultramafic rocks from MUF zone (Tessalina et al., 2016a) is similar to that of the Ordovician MORB from the Urals (Spadea and d'Antonio, 2006). The Uralian MORBs are much more radiogenic compared to the average composition of MORB and oceanic basalts in Northern hemisphere ($\Delta^{207}Pb/^{204}Pb \sim 11$), showing a clear enrichment in radiogenic lead. This enrichment in Urals MORB and peridotites has been ascribed to the variable contributions from a sedimentary component likely made up of pelagic clays (Spadea and d'Antonio, 2006), with most of the data showing intermediate composition between typical MORB and oceanic sediments.

The Ivanovka and Dergamysh host rocks are characterised by relatively low radiogenic Os isotopic composition, with present-day values for mafic and ultramafic rocks not exceeding 0.4 for $^{187}Os/^{188}Os$, with an exception of one highly radiogenic ratio of 7.9 for serpentinite (Gannoun et al., 2003). These values are similar to that obtained for island arc mantle in modern settings. For example, Kamchatka peridotitic xenoliths are having slightly higher Os isotopic composition ($^{187}Os/^{188}Os$) in comparison to the DMM, ranging from 0.12 to 0.5 (e.g., Kepezhinskas and Defant, 2001).

The U-Pb zircon ages reported in this study range from Paleoarchean to Cambrian, and have been probably sourced from much older rocks than Ordovician – Carboniferous volcanics of Magnitogorsk island arc. The possible candidates include Neoproterozic oceanic crust, as recorded for mafic-ultramafic massifs across the Urals. The relics of these massifs have been attributed to belong to earlier Neoproterozoic stages of pre-Uralian ocean development. Alternative sources of radiogenic Os may be old Archean continental crust fragments or sediments sourced from the adjacent East-European continent, or Proterozoic sediments accumulated near the adjacent continent and presently outcropping near the western edge of Urals (Bashkirian anticlinorium).

These older rocks could be available in deeper portions of hydrothermal systems, and contribute into the total metals intake by the hydrothermal fluid. Given that the Re is moderately incompatible, it will be enriched in mafic and/or felsic rocks relative to peridotites, producing radiogenic ^{187}Os isotope over time. The radiogenic Os ingrowth may be estimated using Os decay equation at $^{187}Os/^{188}Os = 4.5$, taking median age of zircons 2176 Ma, $^{187}Re/^{188}Os$ ratio of 120 (close to MORB), and ^{187}Re decay constant of 1.666×10^{-11} year^{-1}.

6.4.5. Source of metals in ores

In an ancient hydrothermal system, it is necessary to take into account the secular increase in ^{187}Os as a result of ^{187}Re decay. The correlation between $^{187}Re/^{188}Os$ and $^{187}Os/^{188}Os$ on the isochron diagram (Gannoun et al., 2003) shows that the Re-Os system has not been perturbed since *ca.* 366 Ma. This allows the calculation of the initial Os isotopic composition at this time (cf. Shirey and Walker, 1998) and of the common Os concentrations (=total Os – radiogenic Os), which correspond to the Os contents at the time of closure of the isotopic system. According to Gannoun et al. (2003), this time corresponds to an episode of metamorphic isotopic resetting during arc-continent collision. This age was recently re-interpreted by Tessalina et al. (2017). Based on Re-Os age similarity with other VHMS deposits from the same metallogenic province, these authors argued that the Re-Os age reflects the latest episode of the multi-stage history of VHMS deposits development.

In the Dergamysh ores, the initial $^{187}Os/^{188}Os$ isotope ratios in the sulphide sandstones are low, ranging from 0.207 to 0.714 (Fig. 15). The lowest value is similar to that of mantle (abyssal peridotite) and chlorite-altered mafic breccia at the hanging wall of the orebody. The hydrothermal massive sulphide breccias are characterized by more variable and, generally, higher initial $^{187}Os/^{188}Os$ isotope ratios (0.602–4.332) and lower initial Os contents. This trend can reflect mixing of a high-Os, unradiogenic mantle-derived component (peridotite and/or mafic rocks) with a low-Os, more radiogenic component (see Fig. 15). This component may be attributed either to magmatic fluid, either to subduction-related fluid released during the subduction of adjacent continent. The subduction-related fluid is unlikely candidate for radiogenic Os component, because the Pb isotope compositions of the Dergamysh ores and host rocks are similar to that of Ordovician Urals MORBs, and dissimilar to that of the deposits in arc and fore-arc setting (Tessalina et al., 2016a). Osmium and sulphur isotopic composition of magmatic fluid in fore-arc setting would be similar to that of mantle (mantle-derived basalts), and, consequently, unradiogenic for Os and close to 0‰ for S. However, the disproportionation of H_2S gas would create light sulphur, which was observed for Dergamysh ores and could be potentially attributed to such processes. However, the magmatic fluid is more typical for felsic

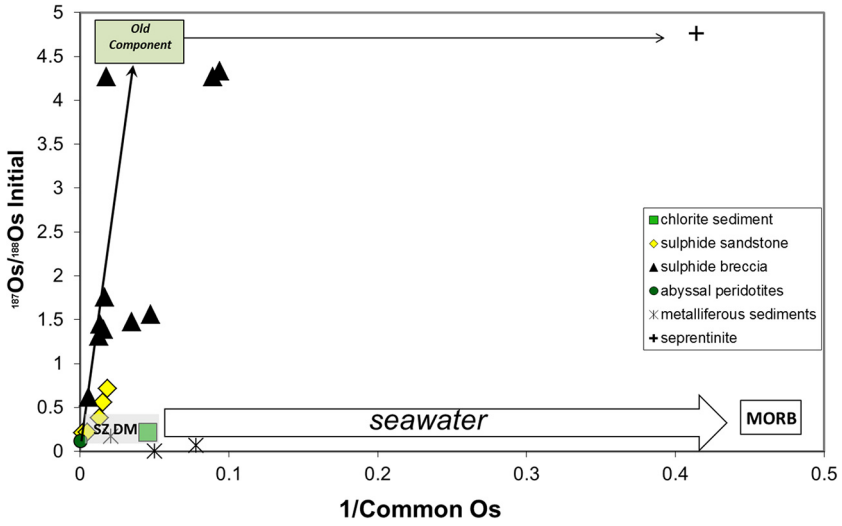

Fig. 15. 1/Common Os vs intial $^{187}Os/^{188}Os$ for the Dergamysh ores. Data are recalculated from Gannoun et al. (2003) at 366 Ma, i.e. at the time of Re-Os system closure. Note that the Upper Devonian seawater end-member is out of scale because of the low Os contents; its Os isotopic composition is inferred to be low radiogenic (*ca.* 0.2–0.45, see text for details). Radiogenic Os end-member was estimated based on Proterozoic age of ca. 2.1 Ga and $^{187}Re/^{188}Os$ ratio of 160. The radiogenic ^{187}Os ingrowth of this rock since Proterozoic will result in $^{187}Os/^{188}Os$ of 4.5.

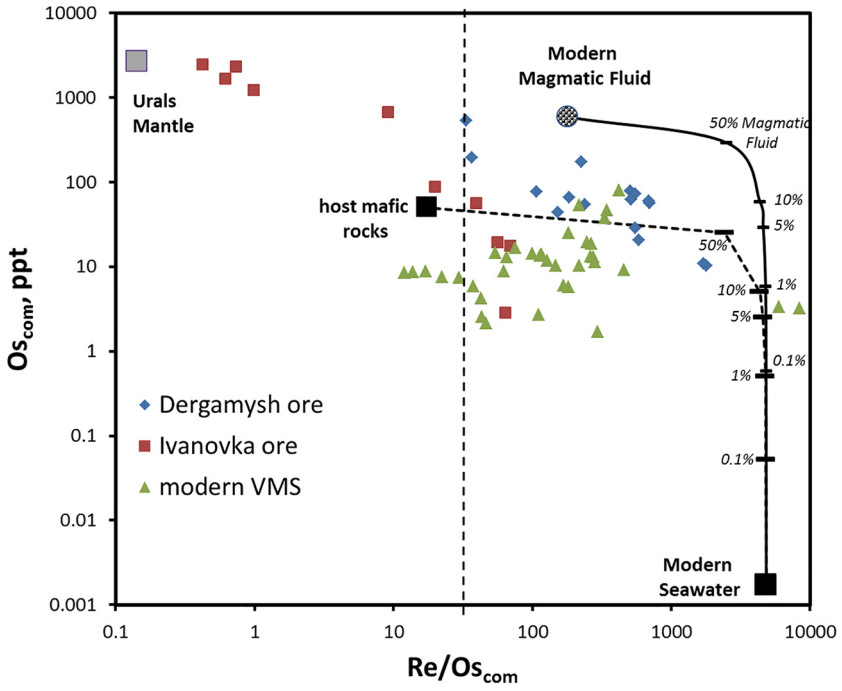

Fig. 16. Re/Os_{com} versus Os_{com} mixing diagram, showing initial Re and Os compositon at time of formation of Dergamysh and Ivanovka ores (data from Gannoun et al., 2003), and compositions of possible end-members components: seawater (Sharma et al., 2000), host mafic rocks (Gannoun et al., 2003), Urals mantle (Tessalina et al., 2007), magmatic fluid in modern supra-subduction zone setting (Tessalina et al., 2008, and Yudovskaya et al., 2008).

magmas and not expected to be a dominant source of metals in MUF zone setting. The most possible candidate for radiogenic Os would be the Precambrian rocks which became radiogenic over time. The presence of such an old rocks is confirmed by Archean to Cambrian U-Pb ages of zircons in Dergamysh host rocks from this study.

The input of different end-members (mantle, seawater, magmatic fluid) in metals budget may be also tested using Re vs. Os systematics, due to the slightly different geochemical behaviour of these elements. During mantle melting, Os behaves as a compatible element and is preferentially retained in the residue, while Re is moderately incompatible and is preferentially incorporated into melts (e.g., Shirey and Walker, 1998), creating a difference over time between residue (e.g., peridotite) and melts (e.g., basalts). Re and Os contents in modern supra-subduction zone magmatic fluids have been studied by Tessalina et al. (2008a) and Yudovskaya et al. (2008) and can be used to approximate those in Devonian time. These fluids have similar Re/Os ratios as the associated hydrothermal sulphides but distinctly higher Os abundances (Fig. 16). In the Re/Os versus Os mixing diagram (Fig. 16), the Dergamysh sulphides have slightly higher Os contents at the same Re/Os ratios compared with modern mafic-ultramafic hosted

deposits (Zeng et al., 2014) and fall in an intermediate field between mafic host-rocks, seawater and the average supra-subduction zone magmatic fluid. The Ivanovka sulphides scatter from compositions approaching that of Urals mantle rocks (i.e., low Re/Os and high Os) to compositions similar to those of their host mafic rocks (Fig. 16). Combining initial $^{187}Os/^{188}Os$ vs. Os_{com} and Re/Os_{com} vs Os_{com} systematics, it can be concluded that the on-seafloor Dergamysh sulphides most probably inherited their Re and Os from their mafic-ultramafic substrate with variable contributions from seawater (Fig. 16). Based on Re/Os_{com} vs Os_{com} systematics, the sub-seafloor Ivanovka sulphides appear to have been more influenced by their ultramafic substrate components and less influenced by seawater (Fig. 16).

7. Conclusions

The HSEs contents in the studied Dergmaish and Ivanovka deposits in a suture zone setting are characterised by lower Pt and Pd contents compared to other Urals VHMS deposits in arc setting. In Dergamysh massive sulphides, the PGEs and Au positively correlate with Cu, whereas Pt also correlates with Co. For Ivanovka mainly disseminated ores and host rocks, two trends can be observed: (a) low to high PGE at low Au in rocks, with negative Ni-Pd correlation; and (b) both PGE and Au are variable in ores with significant correlation between Au and Pd. Rhenium contents are lower in the sulphide sandstones from the Dergamysh deposit (from 9 to 19 ppb) than associated sulphide breccia (from 12 to 42 ppb of Re).

Combined Os-Pb-S isotope systematics in the studied hydrothermal system of the Dergamysh deposit is controlled by the mixture of mantle-derived host rocks and seawater with an additional contribution from more radiogenic Os component which can be attributed to ^{187}Os ingrowth of Archean to Proterozoic rocks occurring within the serpentinitic melange and evidenced by old Archean to Palaeozoic U-Pb zircon dating (2.8 Ga to 415 Ma). Such an old zircons may be derived from adjacent East-European continent (Volga-Uralia block), and may indicate the presence of old continental blocks in a base of Urals, as it is a case in some modern island arc systems.

The S isotopic composition varies from −4.6‰ to +1.3‰ of $\delta^{34}S$, which is in line with other mafic-hosted Urals deposits, but rather light compare to average VHMS systems in island arc settings. This light sulphur isotopic composition may be attributed to bacterial reduction processes, which have been described for modern seafloor hydrothermal systems hosted by serpentinites. The disproportionation of magmatic fluid is less likely due to geotectonic setting in nature of the host rock, with magmatic fluids being mostly typical for felsic-hosted VHMS systems.

Acknowledgements

The study is partly founded by MinUrals INCO-COPERNICUS project. Authors acknowledge the significant contributions from T. Augé, B. Bourdon, A. Gannoun and J.-J. Orgeval. Prof. McNaughton is acknowledged for English correction and useful comments. The meticulous reviews from I.Yu. Melekestseva and P. Nimis, as well as the editorial handling by O.Yu. Plotinskaya, greatly improved the manuscript.

References

Andersen, T., 2002. Correction of common Pb in U-Pb analyses that do not report ^{204}Pb. Chem. Geol. 192, 59–79.

Alt, J.C., Shanks, W.C., 1998. Sulphur in serpentinized oceanic peridotites: serpentinization processes and microbial sulfate reduction. J. Geophys. Res. 103, 9917–9929.

Artyushkova, O.V., Maslov, V.A., 2008. Detailed correlation of the Devonian 738 deposits in the South Urals and some aspects of their formation. Bull. Geosci. 739 83(4), Czech Geological Survey, Prague, pp. 391–399.

Bailly, L., Orgeval, J.J., Tesalina, S.G., Zaykov, V.V., Maslennikov, V.V., 1999, Fluid inclusion data of the Alexandrinskoye massive sulfide deposit. Stanley et al. (Eds.), Urals: Mineral Deposits: Processes to Processing, pp. 13–16.

Beane, R.J., Connelly, J.N., 2000. $^{40}Ar/^{39}Ar$, U-Pb, and Sm-Nd constraints on the timing of metamorphic events in the Maksyutov Complex, southern Ural Mountains. J. Geol. Soc., Lond. 157, 811–822.

Borodaevskaya, M.B., Krivtsov, A.I., Shirai, E.P., 1977. Provinces of Massive Sulphide Deposits: Principles of Tectonic Study. Nedra, Moscow (in Russian).

Brazelton, W.J., Schrenk, M.O., Kelley, D.S., Baross, J.A., 2006. Methane- and sulfur-metabolizing microbial communities dominate the Lost City Hydrothermal Field ecosystem. Appl. Environ. Microbiol. 72, 6257–6270.

Brown, D., Spadea, P., 1999. Processes of forearc and accretionary complex Formation during arc-continent collision in the southern Ural Mountains. Geology 27, 649–652.

Brown, D., Alvarez-Marron, J., Pérez-Estaun, A., Puchkov, V., Gorozhanina, Y., Ayarza, P., 2001. Structure and evolution of the Magnitogorsk forearc basin: identifying upper crustal processes during arc-continent collision in the southern Urals. Tectonics 20, 364–375.

Brügmann, G.E., Birck, J.L., Herzig, P.M., Hofmann, A.W., 1998. Os isotopic composition and Os and Re distribution in the active mound of the TAG hydrothermal system, Mid-Atlantic Ridge. Proceed. Ocen Drilling Progr., Sci. Results 158, 91–100.

Brunner, B., Bernasconi, S.M., 2005. A revised isotope fractionation model for dissimilatory sulfate reduction in sulfate reducing bacteria. Geochim. Cosmochim. Acta 69, 4759–4771.

Buys, J., Spandler, C., Holm, R.J., Richards, S.W., 2014. Remnants of ancient Australia in Vanuatu: implications for crustal evolution in island arcs and tectonic development of the southwest Pacific. Geology 42, 939–942.

Cave, R.R., Ravizza, G.E., German, C.R., Thomson, J., Nesbitt, R.W., 2003. Deposition of osmium and other platinum-group elements beneath the ultramafic-hosted Rainbow hydrothermal plume. Earth Planet. Sci. Lett. 210, 65–79.

Chiaradia, M., Fontboté, L., 2001. Radiogenic lead signatures in Au-rich volcanic-hosted massive sulfide ores and associated volcanic rocks of the Early Tertiary Macuchi island arc (Western Cordillera of Ecuador). Econ. Geol. 96, 1361–1378.

Delacour, A., Früh-Green, G.L., Bernasconi, S.M., Kelley, D.S., 2008. Sulfur in peridotites and gabbros at Lost City (30°N, MAR): implications for hydrothermal alteration and microbial activity during serpentinization. Geochim. Cosmochim. Acta 72, 5090–5110.

Dobrovolskaya, M.G., Distler, V.V., 1998. The noble metals in Cu-massive sulphide deposits of the South Urals. In: International platinum Theophrastus Publication. St.-Petersburg - Athens, pp. 155–171.

Drummond, S.E., Ohmoto, H., 1985. Chemical evolution and mineral deposition in boiling hydrothermal systems. Econ. Geol. 80, 126–147.

Dubinina, S.V., Ryazantsev, A.V., 2008. Conodont stratigraphy and correlation of the Ordovician volcanogenic and volcanogenic sedimentary sequences in the South Urals. Russ. J. Earth Sci. 10 (5), 1–31.

Eremin, N.I., Sergheeva, N.I., Shishakov, V.B., 1997. The occurence of palladium-bearing melonit in the copper sulphide ore of Pishminsko-Kluchevskoe deposit in the Ural. Doklady Acad. Nauk 355 (6), 795–797 (in Russian).

Fershtater, G.B., Krasnobaev, A.A., Bea, F., Montero, P., Levin, V.Y., Kholodnov, V.V., 2009. Isotopic-geochemical features and age of zircons in dunites of the platinum-bearing type Uralian massifs: petrogenetic implications. Petrology 17 (5), 503–520.

Gannoun, A., Tessalina, S., Bourdon, B., Orgeval, J.-J., Birck, J.-L., Allègre, C.-J., 2003. Re-Os isotopic constraints on the genesis and evolution of the Dergamysh and Ivanovka Cu (Co, Au) massive sulphide deposits, South Urals, Russia. Chem. Geol. 196, 193–207.

Goodfellow, W.D., Blaise, B., 1988. Sulfide formation and hydrothermal alteration of hemipelagic sediment in Middle Valley, northern Juan de Fuca Ridge. Can. Mineral. 26, 675–696.

Goodfellow, W.D., Franklin, J.M., 1993. Geology, mineralogy, and chemistry of sediment-hosted clastic massive sulphides in shallow cores, Middle Valley, northern Juan de Fuca Ridge. Econ. Geol. 88, 2037–2068.

Halter, W.E., Webster, J.D., 2004. The magmatic to hydrothermal transition and its bearing on ore-forming systems. Chem. Geol. 210, 1–6.

Herrington, R.J., Armstrong, R.N., Zaykov, V.V., Maslennikov, V.V., Tessalina, S., Orgeval, J.-J., Taylor, R.N.A., 2002. Massive sulphide deposits in the south Urals: Geological setting within the framework of the Urals orogen. In: Brown, D., Juhlin, C., Puchkov, V. (Eds.), Geoph. Monograph Series, vol. 132, pp. 155–182.

Herrington, R.J., Zaykov, V.V., Maslennikov, V.V., Brown, D., Puchkov, V.N., 2005. Mineral Deposits of the Urals and Links to Geodynamic Evolution. In: Hedenquist et al. (Eds.), Economic Geology 100th Anniversary Volume, pp. 1069–1095.

Herzig, P.M., Hannington, M.D., Arribas Jr., A., 1998. Sulfur isotopic composition of hydrothermal precipitates from the Lau backarc: implications for magmatic contributions to seafloor hydrothermal systems. Miner. Deposita 33, 226–237.

Hofmann, A.W., 1997. Mantle geochemistry: the message from oceanic volcanism. Nature 385, 219–229.

Hu, G.X., Rumble, D., Wang, P.L., 2003. An ultraviolet laser microprobe for the in situ analysis of multisulphur isotopes and its use in measuring Archean sulphur isotope mass-independent anomalies. Geochim. Cosmochim. Acta 67 (17), 3101–3118.

Huston, D.I., Pehrsson, P., Eglington, B.M., Zaw, K., 2010. The geology and metallogeny of volcanic-hosted massive sulphide deposits: variations through geologic time and with tectonic setting. Econ. Geol. 105, 571–591.
Huston, D.L., Relvas, J.M.R.S., Gemmell, J.B., Drieberg, S., 2011. The role of granites in volcanic-hosted massive sulphide ore-forming systems: an assessment of magmatic–hydrothermal contributions. Miner. Deposita 46, 473–507.
Jackson, S.E., Pearson, N.J., Griffin, W.L., Belousova, E.A., 2004. The application of laser ablation microprobe-inductively coupled plasma-mass spectrometry (LAM-ICPMS) to in situ U-Pb zircon geochronology. Chem. Geol. 211, 47–69.
Kampschulte, A., Strauss, H., 2004. The sulphur isotopic evolution of Phanerozoic seawater based on the analysis of structurally substituted sulfate in carbonates. Chem. Geol. 204, 255–286.
Karpukhina, V.S., Naumov, V.B., Vikentev, I.V., 2013. Genesis of massive sulphide deposits in the Verkhneuralsk ore district, the South Urals, Russia: evidence for magmatic contribution of metals and fluids. Geol. Ore Deposits 55 (2), 125–143.
Kemp, A.I.S., Wormald, R.J., Whitehouse, M.J., Price, R.C., 2005. Hf isotopes in zircon reveal contrasting sources and crystallization histories for alkaline to peralkaline granites of Temora, southeastern Australia. Geology 33, 797–800.
Kennicutt, M.C., Burke, R.A., Macdonald, I.R., Brooks, J.M., Denoux, G.J., Macko, S.A., 1992. Stable isotope partitioning in seep and vent organisms – chemical and ecological significance. Chem. Geol. 101, 293–310.
Kepezhinskas, P., Defant, M.J., 2001. Nonchondritic Pt/Pd ratios in arc mantle xenoliths: evidence for platinum enrichment in depleted island-arc mantle sources. Geology 29, 851–854.
Kim, J., Lee, I., Lee, K.Y., 2004. S, Sr, and Pb isotopic systematics of hydrothermal chimney precipitates from the Eastern Manus Basin, western Pacific: evaluation of magmatic contribution to hydrothermal system. J. Geophys. Res. 109, B12210. http://dx.doi.org/10.1029/2003JB002912.
Kontar, E.S., Libarova, L.E., 1997. The Cu, Zn, Pb Metallogeny in the Urals. // Ekaterinburg: Urals Geological Committee, 1997. 233 p (in Russian).
Koroteev, V.A., de Boorder, H., Netcheukhin, V.M., Sazonov, V.N., 1997. Geodynamic setting of the mineral deposits of the Urals. Tectonophysics 276, 291–300.
Kovalev, S.G., Puchkov, V.N., Salikhov, D.N., 2015. New data on platinum group elements in sulphide deposits of the South Urals. Dokl. Earth Sci. 464 (1), 898–902.
Labidi, J., Cartigny, P., Moreira, M., 2013. Non-chondritic sulphur isotope composition of the terrestrial mantle. Nature 501, 208–211.
Ludwig, K.R., 2003. User's manual for Isoplot 3.00: A Geochronological Toolkit for Microsoft Excel. Kenneth R. Ludwig.
Malitch, K.N., Efimov, A.A., Ronkin, Yu.L., 2009. Archean U-Pb isotope age of zircon from dunite of the Nizhny Tagil massif (Platinum Belt of Urals). Doklady Earth Sci. 427(5), 851–855 (translated from Doklady Akademii Nauk 427 (1), 101–105).
Marschall, H.R., Shimizu, N., 2012. Sulphur Isotopes in High-pressure Rocks. Goldschmidt Conference Abstracts, #2516.
Mathur, R., Ruiz, J., Tornos, F., 1999. Age and sources of the ore at Tharsis and Rio Tinto, Iberian Pyrite Belt, from Re–Os isotopes. Miner. Depos. 34, 790–793.
McDonough, W.F., Sun, S.-S., 1995. The composition of the Earth. Chem. Geol. 120, 223–253.
McKibben, M.A., Eldridge, C.S., 1990. Radical sulfur isotope zonation of pyrite accompanying boiling and epithermal gold deposition: a SHRIMP study of the Valles Caldera, New Mexico. Econ. Geol. 85, 1917–1925.
Melekestseva, I.Yu., Zaykov, V.V., Nimis, P., Tret'yakov, G.A., Tessalina, S.G., 2013. Cu–(Ni–Co–Au)-bearing massive sulphide deposits associated with mafic–ultramafic rocks of the Main Urals Fault, South Urals: geological structures, ore textural and mineralogical features, comparison with modern analogues. Ore Geol. Rev. 52, 18–36.
Mints, M.V., 2011. 3D Model of deep structure of the early precambrian crust in the East European Craton and Paleogeodynamic Implications. Geotectonics 45, 267–290.
Nimis, P., Tesalina, S.G., Omenetto, P., Tartarotti, P., Lerouge, C., 2004. Phyllosilicate minerals in the hydrothermal mafic–ultramafic-hosted massive-sulphide deposit of Ivanovka (southern Urals): comparison with modern ocean seafloor analogues. Contrib. Miner. Petrol. 147 (3), 363–383.
Nimis, P., Zaykov, V.V., Omenetto, P., Melekestseva, I.Yu., Tesalina, S.G., Orgeval, J.-J., 2008. Peculiarities of some mafic–ultramafic- and ultramafic-hosted massive sulphide deposits from the Main Uralian Fault Zone, southern Urals. Ore Geol. Rev. 33, 49–69.
Nimis, P., Omenetto, P., Buschmann, B., Jonas, P., Simonov, V.A., 2010. Geochemistry of igneous rocks associated with ultramafic–mafic-hosted Cu (Co, Ni, Au) VMS deposits from the Main Uralian Fault (Southern Urals, Russia). Mineral. Petrol. 100, 201–214.
Novgorodova, M.I., 1976. Platinum, palladium and gold in the Cu-sulphide ore of South Ural Doklady Academy Nauk, vol. 226(4), pp. 942–944 (in Russian).
Ohmoto, H., 1986. Stable isotope geochemistry of ore deposits. In: Valley, J.W. et al. (Eds.), Stable Isotopes in High Temperature Geological Processes. Mineral. Soc. of Am., Washington, D.C., pp. 491–570.
Ohmoto, H., Lasaga, A.C., 1982. Kinetics of reactions between aqueous sulfates and sulfides in hydrothermal systems. Geochim. Cosmochim. Acta 46, 1727–1745.
Pašava, J., Vymazalová, A., Petersen, S., 2007. PGE fractionation in seafloor hydrothermal systems: examples from mafic- and ultramafic-hosted hydrothermal fields at the slow-spreading Mid-Atlantic Ridge. Miner. Depos. 42, 423–431.
Peter, J.M., Shanks, W.C., 1992. Sulphur, carbon, and oxygen isotope variations in submarine hydrothermal deposits of Guaymas Basin, Gulf of California. Geochim. Cosmochim. Acta 56, 2025–2040.
Prokin, V.A., Buslaev, F.P., 1999. Massive copper-zinc sulphide deposits in the Urals. Ore Geol. Rev. 14, 1–69.
Puchkov, V.N., 2017. General Features Relating to the Occurrence of Mineral Deposits in the Urals: What, where, when and why, Ore Geol. Rev., http://dx.doi.org/10.1016/j.oregeorev.2016.01.005.
Puchkov, V.N., 2010. Geology of the Urals and Cis-Urals (actual problems of stratigraphy, tectonics, geodynamics and metallogeny). Design Poligraph Service, Ufa. 280 pp. (in Russian).
Ravizza, G., Martin, C.E., German, C.R., Thompson, G., 1996. Os isotopes as tracers in seafloor hydrothermal systems: metalliferous deposits from the TAG hydrothermal area, 26°N Mid-Atlantic Ridge. Earth Planet. Sci. Lett. 138, 105–119.
Romanyuk, T.V., Maslov, A.V., Kuznetsov, N.B., Belousova, E.A., Ronkin, Yu.L., Krupenin, M.T., Gorozhanin, V.M., Gorozhanina, E.N., Seregina, E.S., 2013. First data on LA-ICP-MS U/Pb zircon geochronology of Upper Riphean sandstones of the Bashkir Anticlinorium (South Urals). Dokl. Earth Sci. 452 (2), 997–1000.
Savelieva, G.N., Sharaskin, A.Ya., Saveliev, A.A., Spadea, P., Gaggero, L., 1997. Ophiolites of the southern Uralides adjacent to the East European continental margin. Tectonophysics 276, 117–137.
Seravkin, I.B., Znamensky, S.E., Kosarev, A.M., 1994. Volcanic metallogeny of the southern Urals. Nauka, Moscow, 152 pp (in Russian).
Seravkin, I.B., Znaminsiy, S.E., Kosarev, A.M., 2001. Fault Tectonics and Ore Deposits of the Trans-Uralian Bashkiria. Poligrafcombinat, Ufa (in Russian).
Seyfried, W.E., Ding, K., 1995. Phase equilibria in subseafloor hydrothermal system: a review of the role of redox, temperature, pH and dissolved Cl on the chemistry of hot spring fluids at mid-ocean ridges, in Seafloor Hydrothermal Systems: Physical, Chemical, Biological, and Geological Interactions. In: Humphris, S.E. et al. (Eds.), Geophysical Monograph Series 91, AGU, Washington, D.C., pp. 248–272.
Shanks, W.C., 2001. Stable Isotopes in Seafloor Hydrothermal Systems: Vent fluids, hydrothermal deposits, hydrothermal alteration, and microbial processes. Rev. Mineral. Geochem. 43 (1), 469–525.
Shanks, W.C., 2003. Stable isotope in seafloor hydrothermal systems. In: Valley, J.W., Cole, D.R. (Eds.), Stable Isotope Geochemistry, vol. 43. Reviews in Mineralogy and Geochemistry. Mineralogical Society of America, pp. 469–525.
Sharma, M., Wasserburg, G.J., Hofmann, A.W., Butterfield, D.A., 2000. Osmium isotopes in hydrothermal fluids from the Juan de Fuca Ridge. Earth Planet. Sci. Lett. 179, 139–152.
Shirey, S.B., Walker, R.J., 1998. The Re-Os isotope system in cosmochemistry and high-temperature geochemistry. Annu. Rev. Earth Planet. Sci. 26, 423–500.
Spadea, P., d'Antonio, M., 2006. Initiation and evolution of intra-oceanic subduction in the Uralides: geochemical and isotopic constrains form Devonian oceanic rocks of the Southern Urals, Russia. Island Arc 15, 7–25.
Spadea, P., Antonio, M.D., Kosarev, A., Gorozhanina, Y., Brown, D., 2002. Arc-continent collision in the Southern Urals: petrogenetic aspects of the forearc-arc complex. In: Brown, D., Juhlin, C., Puchkov, V. (Eds.) Geoph. Monograph Series 132, pp. 101–134.
Tapster, S., Roberts, N.M.W., Petterson, M.G., Saunders, A.D., Naden, J., 2014. From continent to intra-oceanic arc: Zircon xenocrysts record the crustal evolution of the Solomon island arc. Geology 42, 1087–1090.
Tatsumoto, M., 1969. Lead isotopics in volcanic rocks and possible ocean-floor thrusting beneath island arcs. Earth Planet. Sci. Lett. 6, 369–376.
Tesalina, S., Nimis, P., Augé, T., Zaykov, V., 2003. Origin of chromite in mafic–ultramafic-hosted hydrothermal massive sulphides from the Main Uralian Fault, South Urals. Russia. Lithos 70 (1–2), 39–59.
Tessalina, S.G., Herrington, R.J., Taylor, R.N., Sundblad, K., Maslennikov, V.V., Orgeval, J.-J., 2016a. Lead isotopic systematics of massive sulphide deposits in the Urals: applications for geodynamic setting and metal sources. Ore Geol. Rev. 72, 22–36.
Tessalina, S.G., Malitch, K.N., Auge, T., Puchkov, V.N., Belousova, E., McInnes, B.I.A., 2016b. Origin of the Nizhny Tagil clinopyroxenite-dunite massif (Uralian Platinum Belt, Russia): insights from PGE and Os isotope systematics. J. Petrol., 1–21
Tessalina, S.G., Jourdan, F., Belogub, E.V., 2017. Significance of Late Devonian – Lower Carboniferous ages of hydrothermal sulphides and sericites from the Urals Volcanic-Hosted Massive Sulphide deposits. Ore Geol. Rev. http://dx.doi.org/10.1016/j.oregeorev.2016.08.005.
Tessalina, S.G., Yudovskaya, M.A., Chaplygin, I.V., Birck, J.-L., Capmas, F., 2008a. Sources of unique rhenium enrichment in fumaroles and sulphides at Kudryavy volcano. Geochim. Cosmochim. Acta 72, 889–909.
Tessalina, S., Bourdon, B., Maslennikov, V.V., Orgeval, J.-J., Birck, J.-L., Gannoun, A., Capmas, F., Allègre, C.-J., 2008b. Os isotope distribution within Paleozoic seafloor hydrothermal system in Southern Urals, Russia. Ore Geol. Rev. 33, 70–80.
Tessalina, S.G., Bourdon, B., Gannoun, A., Capmas, F., Birck, J.-L., Allègre, C.J., 2007. Complex Proterozoic to Paleozoic history of the upper mantle recorded in the Urals lherzolite massifs by Re–Os and Sm–Nd systematics. Chem. Geol. 240, 61–84.
Tessalina, S.G., Zaykov, V.V., Orgeval, J.-J., Augé, T., Omenetto, P., 2001. Mafic-ultramafic hosted massive sulphide deposits in Southern Urals (Russia). Proceeding of the joint sixth biennial SGA-SEG meeting. Krakow, pp. 353–356.
Turgeon, S.C., Creaser, R.A., Algeo, T.J., 2007. Re–Os depositional ages and seawater Os estimates for the Frasnian-Famennian boundary: implications for weathering rates, land plant evolution, and extinction mechanisms. Earth Planet. Sci. Lett. 261, 649–661.

Vikentev, I.V., Yudovskaya, M.A., Moloshag, V.P., 2006. Speciation of noble metals and conditions of their concentration in massive sulphide ores of the Urals. Geol. Ore Deposits 48, 77–107.
Vikentev, I.V., Moloshag, V.P., Yudovskaya, M.A., Eremin, N.I., 2002. Platinum group elements in ores of massive sulphide deposits of the Urals. Dokl. Earth Sci. 385 (5), 488–492.
Vikentyev, I.V., Yudovskaya, M.A., Mokhov, A.V., Kerzin, A.L., Tsepin, A.I., 2004. Gold and PGE in massive sulphide ore of the Uzelginsk deposit, Southern Urals, Russia. Canad. Mineral. 42, 651.
Volchenko, Y.A., Koroteev, V.A., Zoloev, K.K., 1993. Efficiency of Platinum-bearing Belt of the Urals. Yearbook of IGG. Ekaterinburg, pp. 89–92 (in Russian).
Wiedenbeck, M., Allé, P., Corfu, F., Griffin, W.L., Meier, M., Oberli, F., von Quadt, A., Roddick, J.C., Spiegel, W., 1995. Three natural zircon standards for U-Th-Pb, Lu-Hf, trace element and REE analyses. Geostandards Newslett. 19, 1–23.
Yudovskaya, M.A., Tessalina, S., Distler, V.V., Chaplygin, I.V., Chugaev, A.V., Dikov, Y. P., 2008. Behavior of highly-siderophile elements during magma degassing: a case study at the Kudryavy volcano. Chem. Geol. 248, 318–341.
Yushko-Zakharova, 1975. PGE prospects of ore deposits. Moscow, Nedra, 248 pp. (in Russian).
Zaykov, V.V., Maslennikov, V.V., Zaykova, E.V., Herrington, R.J., 1996. Hydrothermal activity and segmentation in the Magnitogorsk – West Mugodjarian zone on the margins of the Urals paleo-ocean. In: Tectonic, Magmatic, Hydrothermal and biological segmentation of the Mid Ocean Ridges, London, pp. 199–210.
Zeng, Z., Chen, S., Selby, D., Yin, X., Wang, X., 2014. Rhenium-Osmium abundance and isotopic compositions of massive sulphides from modern deep-sea hydrothermal systems: implications for vent associated ore forming processes. Earth Planet. Sci. Lett. 396, 223–234.
Zierenberg, R.A., Koski, R.A., Morton, J.L., Bouse, R.M., 1993. Genesis of massive sulphide deposits on a sediment-covered spreading center, Escanaba Trough, southern Gorda Ridge. Econ. Geol. 88, 2069–2098.
Zonenshain, L.P., Korinevsky, V.G., Kuzmin, D.M., Pechersky, D.M., Khain, V.V., Matveenkov, V.V., 1984. Plate tectonic model of the South Urals. Tectonophysics 109, 95–135.